SRR-CWDA-2011-00188
Revision 0

Uncertainty and Sensitivity Analyses for Saltstone Disposal Facility Performance Assessment Case A and Alternative Sensitivity Case K

January 2012

Prepared by: Savannah River Remediation LLC
Closure and Waste Disposal Authority
Aiken, SC 29808

Prepared for U.S. Department of Energy Under Contract No. DE-AC09-09SR22505

APPROVALS

Author:

Richard E. Sheppard
Savannah River Remediation LLC
Closure & Waste Disposal Authority

1/5/2012
Date

Technical Review:

Barry Lester
Savannah River Remediation LLC
Closure & Waste Disposal Authority

1/5/2012
Date

Management Approval:

Kent Rosenberger
Savannah River Remediation LLC
Closure & Waste Disposal Authority

1/10/2012
Date

TABLE OF CONTENTS

LIST OF FIGURES

LIST OF TABLES

ACRONYMS

DOE	U.S. Department of Energy
FDC	Future Disposal Cell
GBM	Gradient Boosting Model
MOP	Member of the Public
NRC	U.S. Nuclear Regulatory Commission
PA	Performance Assessment
RAI	Request for Additional Information
SA	Sensitivity Analysis
SDF	Saltstone Disposal Facility
SI	Sensitivity Indices
UA	Uncertainty Analysis

1.0 INTRODUCTION

A performance assessment (PA) has been completed for the Saltstone Disposal Facility (SDF), SRR-CWDA-2009-00017. During SDF PA review, the U.S. Nuclear Regulatory Commission (NRC) provided two sets of requests for additional information (RAIs). The first set, issued March 31, 2010 via letter from P. M. Bubar to T. Gutmann (ML100820097), was responded to via SRR-CWDA-2010-00033. The second set (RAI-2009-02), issued December 15, 2010 via letter from D. L. Skeen to T. Gutmann (ML103400571), was responded to via SRR-CWDA-2011-00044 Revision 0. In response to a number of RAIs in the second set, Alternative Sensitivity Case K was developed, and described in the response to RAI PA-8 provided in SRR-CWDA-2011-00044 Revision 1. In the RAI PA-8 response, Alternative Sensitivity Case K was analyzed using the PORFLOW model to obtain water concentrations of radioactive contaminants. These concentrations were input into a dose calculator submodel within the GoldSim model to estimate radiological doses to the member of the public (MOP) and the intruder. These radiological doses were presented in the response to RAI PA-8.

To evaluate Alternative Sensitivity Case K further, uncertainty and sensitivity analyses (UA/SA) have been conducted using an updated Stochastic Fate and Transport Model using the GoldSim systems analysis software package. This updated Stochastic Fate and Transport Model was developed to include Alternative Sensitivity Case K specific parameters obtained from PORFLOW. The development of this updated Stochastic Fate and Transport Model is documented in SRR-CWDA-2011-00178 and is identified as GoldSim model file, SRS Saltstone v3.002.gsm (SRR-CWDA-2011-00189), hereinafter referred to as GoldSim v3.002. The benchmarking of GoldSim v3.002 Alternative Sensitivity Case K to the results from PORFLOW is also documented in SRR-CWDA-2011-00178. Because of model refinements made in GoldSim v3.002, benchmarking of SDF PA Case A (Base Case) to the PORFLOW results was redone and is also documented in SRR-CWDA-2011-00178.

This document provides the UA/SA conducted for SDF PA Case A and Alternative Sensitivity Case K using the GoldSim file: SRS Saltstone v3.001.gsm (hereinafter referred to as GoldSim v3.001). GoldSim v3.001 differs from GoldSim v3.002 in some refinements made during the checking and benchmarking process. An assessment has been made comparing the potential impact on the estimate of dose to the MOP between GoldSim v3.001 and v3.002 and is documented in SRR-CWDA-2011-00178. This assessment concludes that the UA/SA conducted using GoldSim model v3.001 is expected to be representative of SDF conceptual model for SDF PA Case A and Alternative Sensitivity Case K. The UA/SA conducted for SDF PA Case A using the SDF PA version of the GoldSim Stochastic Fate and Transport Model (GoldSim v2.009) are provided in Sections 5.6.4 and 5.6.5 of SRR-CWDA-2009-00017.

2.0 PARAMETERS EVALUATED IN THE UA/SA

Section 5.6.3 the SDF PA discusses the parameters evaluated in the UA/SA. Because of the refinements made in GoldSim v3.001, a number of stochastic parameters were modified from those described in SDF PA Section 5.6.3. In addition, the inclusion of Alternative Sensitivity Case K into GoldSim v3.001 required additional stochastic parameters for evaluation. Section 2.1 addresses those stochastic elements that are modified from the elements described in SDF PA Section 5.6.3 that are not case specific. Section 2.2 addresses those stochastic elements that are included in GoldSim v3.001 for Alternative Sensitivity Case K only. Note that because this UA/SA is evaluated for SDF PA Case A and Alternative Sensitivity Case K separately, there is no "All Cases" evaluation; thus, the stochastic element for case scenarios presented in SDF PA Section 5.6.3.1 is not pertinent to this analysis and has not been re-evaluated at this time.

2.1 Stochastic Elements Modified from the SDF PA Analyses

2.1.1 Saturated Zone Width and Thickness

The SDF PA Section 5.6.3.8.1 describes the stochastic elements for the width and thickness of the saturated zone used in the SDF PA analysis. In this refined transport model no uncertainty for the width of the saturated zone is considered since the width of the saturated zone is defined as the width of Vaults 1 and 4 (600 feet) and the diameter (150 feet) of a future disposal cell (FDC). The thickness of the saturated zone in the refined, GoldSim model is based on mixing zone thickness, estimated from cross-sectional diagrams of results from the PORFLOW model results, and is described in SRR-CWDA-2011-00178. The stochastic element for the thickness of the saturated zone is a normal distribution with a mean of 20 meters, a standard deviation of 2.8 meters, a minimum of 12 meters, and a maximum of 28 meters.

2.1.2 Saturated Zone Darcy Velocity

Section 5.6.3.8.2 of the SDF PA describes the stochastic element for the saturated zone Darcy velocity, which assumed that the distribution was independent of the disposal unit. In the refined GoldSim model, the Darcy velocity is dependent on the disposal unit, based on PORFLOW results. Details associated with this stochastic is provided in SRR-CWDA-2011-00178.

2.2 Stochastic Elements Modified for Alternative Sensitivity Case K

2.2.1 Radionuclide Inventory

Section 5.6.3.2 of the SDF PA describes the stochastic elements associated with the inventory in the disposal units. The variability of inventory by source and location has not changed from that described in the SDF PA; however, the average (or deterministic) value for a number of radionuclides have changed in Vault 4 and in the FDCs, as shown in Table 2.2-1. Also shown in Table 2.2-1 are the values that were used in GoldSim v3.001 that are different from the values used in GoldSim v3.002. The inventory differences between GoldSim v3.001 and v3.002 do not significantly influence the results of the UA/SA as discussed below.

Table 2.2-1: Average Inventory for SDF PA Case A and Alternative Sensitivity Case K

Radio-nuclide	Vault 4 Inventory (curies)		FDC (Vault 2, in model) Inventory (curies)	
	Case A (a)	Case K (RAI PA-8)	Case A (b)	Case K (RAI PA-8)
Pu-238	9,100 [9,300] (c)	1,000	No change	No change
U-234	26	10	No change	No change
Th-230	7.5	0.01	0.19 [1.3E-04]	1.3E-04 [0.19]
Ra-226	4.1	0.001	7.8E-07 [1.3E-5]	1.3E-5 [7.8E-07]

(a) Provided in PA Table 3.3-3
(b) Provided in PA Table 3.3-5
(c) Value within [ ] is used in GoldSim v3.001

The inadvertent transcription errors in the inventories for SDF PA Case A and Alternative Sensitivity Case K in GoldSim v3.001, shown in Table 2.2-1, were investigated in SRR-CWDA-2011-00178, and found to have no appreciable impact on the predicted dose in SDF PA Case A or in Alternative Sensitivity Case K. The dose results from SDF PA Case A are dominated by the release of Ra-226 from Vault 4 and the release of Ra-226 is primarily driven by the decay of Th-230. Even though the inventory of Th-230 in the FDCs is significantly reduced from the SDF PA Case A inventory the dominance of the release from Vault 4 compensates for this reduction in the FDC inventory. The dose results from Alternative Sensitivity Case K are dominated by the release of I-129, Cs-134, and Tc-99, which are not impacted by the inventory of Th-230 and Ra-226.

2.2.2 Distribution Coefficient Values

Section 5.6.3.3 of the SDF PA describes the variability for the K_d values. For Alternative Sensitivity Case K a number of K_d values were updated to reflect the latest documented values. These values are provided in the response to RAI PA-8 and are repeated in SRR-CWDA-2011-00178. The variability of the K_d values described in SDF PA Section 5.6.3.3 are retained for Alternative Sensitivity Case K, except for technetium K_d in cementitious materials. A "shrinking core" model is utilized for the change in K_d value as the cementitious material oxidizes and is described in the response to RAI PA-8. The variability of the "shrinking core" K_d analysis is modeled with a scalar applied to the K_d time distribution. This scalar value is assumed to have a lognormal distribution with a geometric mean of 1 and a geometric standard deviation of 1.187 with a minimum value of 0.25 and a maximum value of 1.75.

2.2.3 Transition Times between Chemical States

Section 5.6.3.4 of the SDF PA describes the stochastic elements for the pore volumes used to determine the transition time of the chemical states of the cementitious materials used in the SDF PA analysis. The pore volume required to transition the cementitious materials for Alternative Sensitivity Case K from Region II reducing to Region II oxidizing conditions, and from Region II oxidizing to Region III oxidizing, have been modified. The required pore volumes for transitions have been modified based on revised calculations conducted in response to RAIs PA-8 and SP-8, presented in SRR-CWDA-2011-00044. The stochastic elements for transition volumes are assumed as triangular distributions as used in the SDF PA analysis.

The "most likely" values for Alternative Sensitivity Case K are the values used in the PORFLOW run described in RAI PA-8. For saltstone, the "most likely" value of 505 pore volumes, based on a very conservative value for the reduction capacity of saltstone (0.206 meq e^-/g rather than 0.822 meq e^-/g) and a corrected value for saltstone porosity, is used for the transition from Region II reducing to Region II oxidizing. Applying the same porosity correction, the "most likely" value for the transition of saltstone from Region II oxidizing to Region III oxidizing becomes 7,608 pore volumes. The "most likely" values of pore volumes for the transitioning of concrete are unchanged from the SDF PA analysis.

The maximum values for transition volumes are taken to be the values reported in the response to RAI SP-8, and for concrete, the minimum values for transition volumes would be one-half of the maximum values. For saltstone, the minimum value of pore volumes required for the transition from Region II reducing to Region II oxidizing is calculated to be 415 pore volumes based on the analysis conducted to support the response to RAI SP-8 but with the conservative value for reduction capacity of 0.206 meq e^-/g. The minimum value of pore volumes required for saltstone to transition from Region II oxidizing to Region III oxidizing is assumed as one-half of the value reported in the response to RAI SP-8. Table 2.2-2 summarizes the transition pore volume values used in the stochastic analysis.

Table 2.2-2: Chemical Transition Pore Volumes for Alternative Sensitivity Case K

Alternative Sensitivity Case K Chemical Transition Pore Volumes	Most Likely	Minimum	Maximum
Saltstone Region II Reducing to Region II Oxidizing	505 (a)	415 (b)	1,653 (c)
Saltstone Region II Oxidizing to Region III Oxidizing	7,608 (a)	5,606 (d)	11,213 (c)
Concrete Region II Reducing to Region II Oxidizing	3,230 (e)	2,476 (d)	4,953 (c)
Concrete Region II Oxidizing to Region III Oxidizing	4,206 (e)	3,223 (d)	6,446 (c)

(a) Provided in the response to RAI PA-8
(b) Based on analysis conducted for the response to RAI SP-8 with a conservative value for the reduction capacity of saltstone
(c) Provided in the response to RAI SP-8
(d) One-half of the maximum value
(e) Reported in SDF PA Table 5.6-6

2.2.4 Bioaccumulation Factors and Human Health Exposure Parameters

2.2.4.1 Poultry and Egg Consumption

In response to RAI B-2, presented in SRR-CWDA-2011-00044, two additional pathways were included in the Alternative Sensitivity Case K analysis: poultry consumption and egg consumption. The inclusion of these two pathways to exposure resulted in the addition of six stochastic elements:

1. Poultry consumption rate
2. Egg consumption rate
3. Fraction of local poultry consumed by the MOP
4. Fraction of local poultry consumed by the intruder
5. Fraction of local eggs consumed by the MOP (same as poultry)
6. Fraction of local eggs consumed by the intruder (same as poultry)

The consumption rate of poultry and eggs is based on Table A-1 of ML083190829 and is provided in Table 2.2-3. The fraction of local poultry (or egg) consumed by the MOP or the intruder is based on Table B-1 of ML083190829 and is provided in Table 2.2-3.

Table 2.2-3: Parameters for Poultry and Egg Consumption

Poultry Consumption Rate		**Egg consumption Rate**	
Cumulative Probability	**Value (kg/yr)**	**Cumulative Probability**	**Value (kg/yr)**
0	3.85	0	2.8
0.01	3.85	0.01	2.8
0.05	4.18	0.05	4.5
0.1	5.94	0.1	5.3
0.25	9.57	0.25	8.23
0.5	19.85	0.5	12.36
0.75	38.22	0.75	21.35
0.9	50.83	0.9	35.9
0.95	58.52	0.95	47.35
0.99	72.81	0.99	120.71
1	72.81	1	120.71
Mean	25	Mean	19
Local fraction for MOP (triangular distribution)		**Local fraction for MOP (triangular distribution)**	
Minimum	0.1	Minimum	0.1
Most Likely	0.306	Most Likely	0.306
Maximum	0.5	Maximum	0.5
Local fraction for intruder (triangular distribution)		**Local fraction for intruder (triangular distribution)**	
Minimum	0.1	Minimum	0.1
Most Likely	0.319	Most Likely	0.319
Maximum	0.5	Maximum	0.5

2.2.4.2 Soil Build-up Time

In response to RAI B-3, presented in SRR-CWDA-2011-00044, the radionuclide build-up time for irrigated soil was modified to reflect a value of 25 years with no uncertainty. Thus, for Alternative Sensitivity Case K the soil build-up time is a data element specified as 25 years with no stochastic.

2.2.4.3 Vegetation Production Yield

In response to RAI B-4, presented in SRR-CWDA-2011-00044, the vegetation production yield was updated from 0.7 kg/m^2 (SDF PA Table 5.6-9) to 2.2 kg/m^2 based on SRNL-STI-2010-00447. The stochastic element for this parameter is also based on SRNL-STI-2010-00447 and is a triangular distribution with a most likely value of 2.2 kg/m^2, a minimum value of 0.7 kg/m^2, and a maximum value of 4.0 kg/m^2.

2.3 Uncertainty and Sensitivity Analysis

A special model was developed for performing the UA/SA of the SDF PA Case A and the Alternative Sensitivity Case K calculations using the GoldSim systems analysis software. The model is not intended to predict future potential doses; rather the goal is to characterize the context of uncertainty and sensitivity surrounding the SDF PA calculations.

The UA, discussed in Section 2.3.1, is concerned with how the uncertainty in stochastically defined model input parameters is propagated through the model to the selected model results, or endpoints. These model endpoints are potential radiological doses to hypothetical human receptors and aqueous concentrations of specific radionuclides that have been found to be responsible for those doses.

In contrast, the SA, discussed in Section 2.3.2, is focused on determining which of the many input parameters are most responsible for determining the endpoints.

The probabilistic results from GoldSim v3.001 are used to characterize the uncertainty manifested in the model input distributions. Some of these distributions are parameter values, such as material properties or water flow rates. Others are oriented more toward model uncertainty, such as the stochastic that selects the failure configuration to choose for a given realization. Together, the distributions, defined as stochastic elements in GoldSim, are intended to capture the overall uncertainty in the model. These do not address conceptual model uncertainty, or that induced by model structure, such as discretization.

The UA/SA is based on 5,000 realizations of the GoldSim v3.001 model. The Monte Carlo analysis sampled the input distributions with Latin Hypercube Sampling. Five sets of 1,000 for a given case, but with different seeds, were combined to form one dataset of 5,000 realizations for each of the two case scenarios that were selected for investigation (SDF PA Case A and Alternative Sensitivity Case K).

Note that there is an absence of some model input distributions. From the model's perspective, the definition of an input variable as a single value implies that the value is known perfectly. The consequences of this approach are that the uncertainty shown in the results does not take into account any contributions from such deterministic inputs, thereby potentially underestimating uncertainty.

2.3.1 Uncertainty Analysis

Statistics for maximum values for doses to the MOP and groundwater concentrations are summarized in Tables 2.3-1 and 2.3-2. The values in these tables focus on maximum doses (and concentrations) at general receptor locations, since the relevant performance metric is the maximum dose to the MOP outside the 100-meter buffer zone surrounding the SDF. The values in the tables show summary statistics (mean, median, and 95th percentile) for the maximum values of specific endpoints.

Table 2.3-1: Summary for Selected Endpoints – SDF PA Case A Only

Endpoint	Mean	Median (50th Percentile)	95th Percentile
Maximum MOP dose at any Sector within 10,000 years (mrem/yr)	3.7	3.5	6.0
Maximum MOP dose at any Sector within 20,000 years (mrem/yr)	8.4	7.8	14.2
Maximum MOP dose at Sector B within 10,000 years (mrem/yr)	3.7	3.5	6.0
Maximum MOP dose at Sector B within 20,000 years (mrem/yr)	8.4	7.8	14.2
Maximum MOP dose at Sector J within 10,000 years (mrem/yr)	0.76	0.72	1.3
Maximum MOP dose at Sector J within 20,000 years (mrem/yr)	1.6	1.5	2.6
Maximum aqueous concentration of Tc-99 at Sector B within 20,000 years (pCi/L)	1,280	945	2,730
Maximum aqueous concentration of Tc-99 at Sector J within 20,000 years (pCi/L)	67.2	55.7	160
Maximum aqueous concentration of I-129 at Sector B within 20,000 years (pCi/L)	3.51	3.46	4.81
Maximum aqueous concentration of I-129 at Sector J within 20,000 years (pCi/L)	0.96	0.95	1.32
Maximum aqueous concentration of Ra-226 at Sector B within 20,000 years (pCi/L)	6.0	5.8	8.6
Maximum aqueous concentration of Ra-226 at Sector J within 20,000 years (pCi/L)	0.020	0.019	0.033
Results are based on analysis of 5,000 realizations for SDF PA Case A.			

Table 2.3-2: Summary for Selected Endpoints – Alternative Sensitivity Case K Only

Endpoint	Mean	Median (50th Percentile)	95th Percentile
Maximum MOP dose at any Sector within 10,000 years (mrem/yr)	21.9	20.9	34.6
Maximum MOP dose at any Sector within 20,000 years (mrem/yr)	128	121	205
Maximum MOP dose at Sector B within 10,000 years (mrem/yr)	18.1	17.3	28.8
Maximum MOP dose at Sector B within 20,000 years (mrem/yr)	102	96.9	161
Maximum MOP dose at Sector G within 10,000 years (mrem in a year)	21.8	20.8	34.5
Maximum MOP dose at Sector G within 20,000 years (mrem/yr)	128	121	204
Maximum aqueous concentration of Tc-99 at Sector B within 20,000 years (pCi/L)	43,600	42,700	57,300
Maximum aqueous concentration of Tc-99 at Sector G within 20,000 years (pCi/L)	60,000	58,800	78,800
Maximum aqueous concentration of I-129 at Sector B within 20,000 years (pCi/L)	57.3	55.9	80
Maximum aqueous concentration of I-129 at Sector G within 20,000 years (pCi/L)	79.1	77.2	111
Maximum aqueous concentration of Ra-226 at Sector B within 20,000 years (pCi/L)	10.9	10.2	20.8
Maximum aqueous concentration of Ra-226 at Sector G within 20,000 years (pCi/L)	3.2	2.7	7.1
Results are based on analysis of 5,000 realizations for Alternative Sensitivity Case K.			

To evaluate model uncertainty further, the statistics around the results of interest as a function of time are provided in the following graphs. Note that the results provided in these time history graphs are based on runs of 1,000 realizations rather than the combined set of 5,000 realizations that were used to develop the statistics shown in Tables 2.3-1 and 2.3-2. Therefore, there may not be direct correlation of the graphical results to the tabular results.

Figure 2.3-1 shows the statistics surrounding a MOP dose for Sector B, SDF PA Case A, within 20,000 years. The maximum value of this dose is an endpoint recorded in the tables above. The statistical summary shows the percentiles of the results at any given time. That is, a single time-step would be read by placing a vertical line across the graph. Along that

line, the curves showing percentiles identify the percentile of the MOP dose for Sector B, SDF PA Case A, at that time. Figure 2.3-2 shows analogous information for Sector J, SDF PA Case A.

Figure 2.3-1: Time History of MOP Dose Statistics, Sector B for 20,000 Years – SDF PA Case A

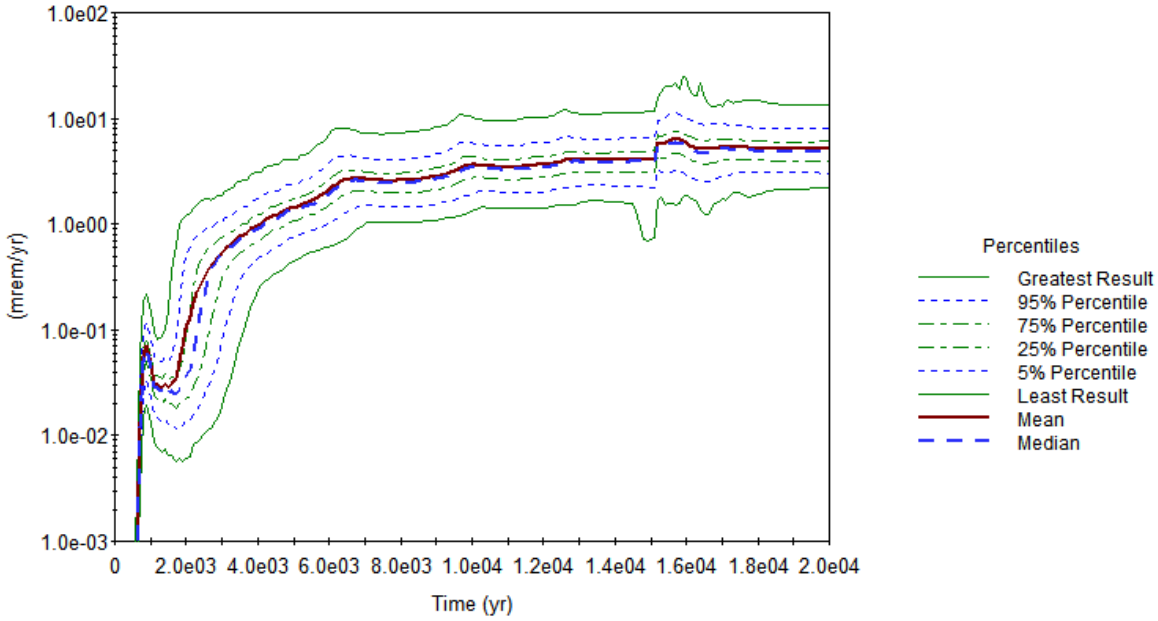

Figure 2.3-2: Time History of MOP Dose Statistics, Sector J for 20,000 Years – SDF PA Case A

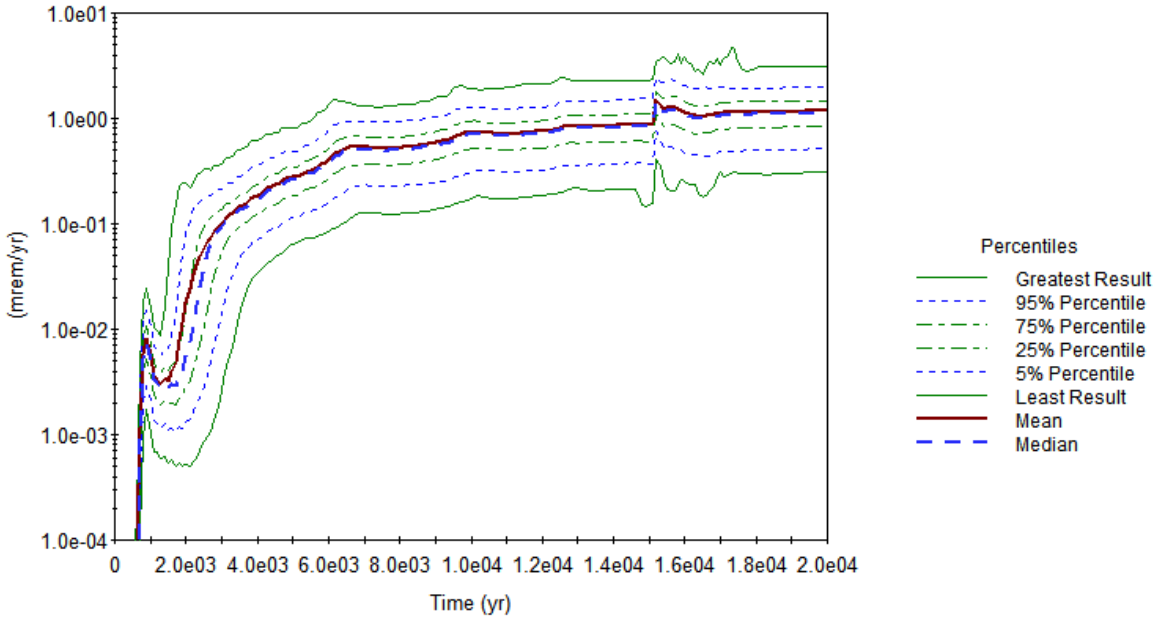

For Alternative Sensitivity Case K, Sectors B and G are examined in Figures 2.3-3 and 2.3-4. Sector G produces the overall maximum values for the dose to the MOP for Alternative Sensitivity Case K.

Figure 2.3-3: Time History of MOP Dose Statistics, Sector B for 20,000 Years – Alternative Sensitivity Case K

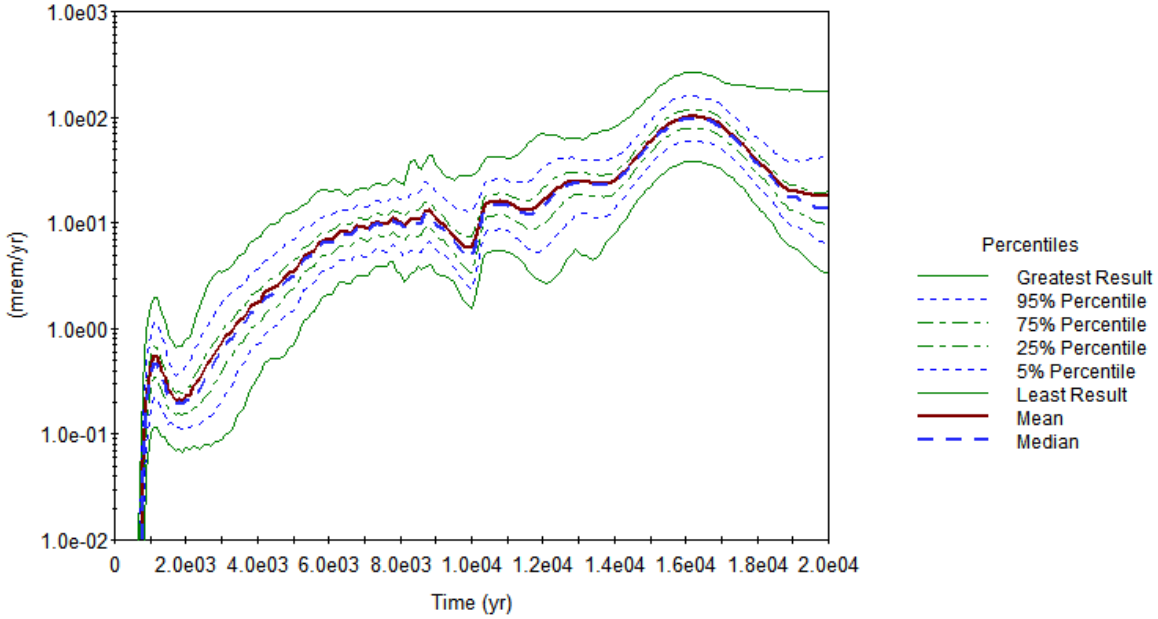

Figure 2.3-4: Time History of MOP Dose Statistics, Sector G for 20,000 Years – Alternative Sensitivity Case K

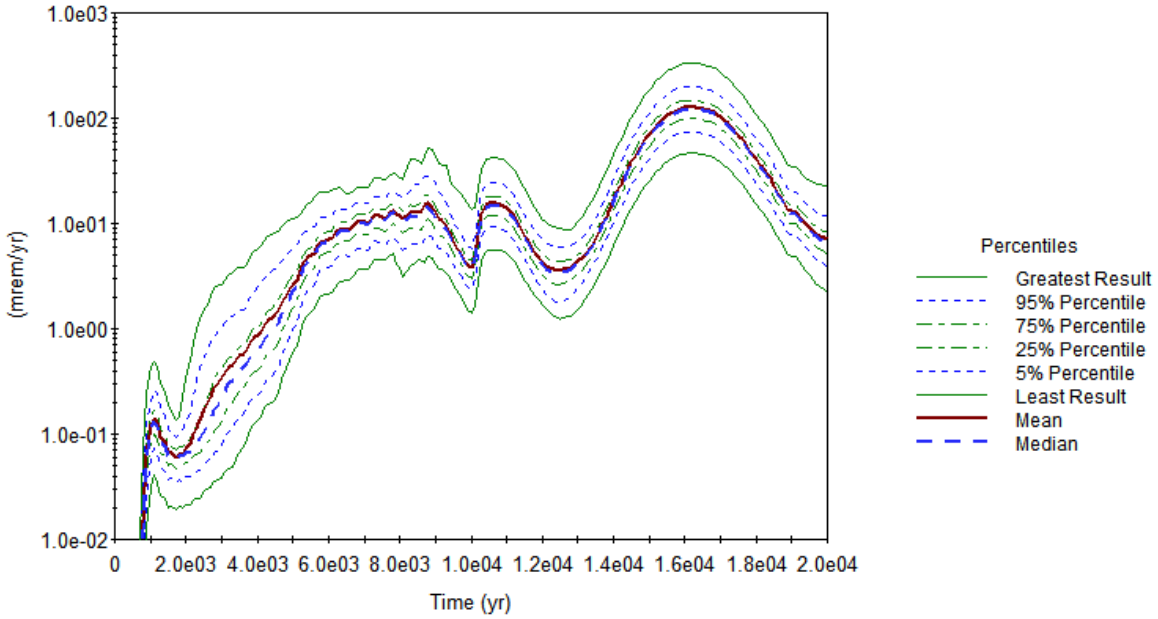

Note that the information presented in the tables and the information in the time history graphs do not present the same information. The tables show summary statistics for maximum doses to the MOP (and aqueous concentrations) achieved over a specified time interval. These are functions (e.g. mean, median, and other percentile) of the maximum values, no matter when that maximum was achieved within the period. Each time step within a realization produces a maximum value. Each realization results in a maximum value achieved over time for the selected endpoints. The mean of these maximum values is the mean of the maximum values averaged over all the realizations.

Figure 2.3-5 shows the mean dose to the MOP, for the SDF PA Case A, located in each of the defined PORFLOW sectors (Sectors A through L), at any point in time, for 20,000 years.

Figure 2.3-5: Mean Dose to a MOP by Sector within 20,000 Years – SDF PA Case A

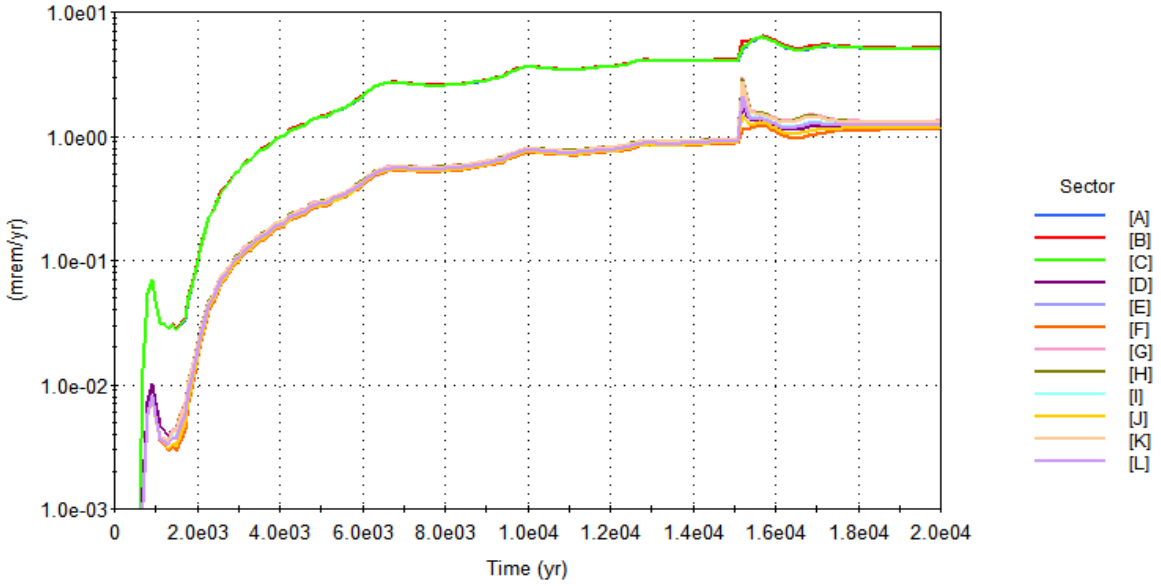

For SDF PA Case A, the dose time histories fall into two distinct groups, the MOP doses seen in Sectors A, B, and C are all nearly identical, and are consistently higher, by one order of magnitude, than the doses seen for Sectors D through L. Doses seen at Sector B are generally the highest, and these are chosen for a more detailed presentation below.

Figure 2.3-6 shows the mean dose to the MOP located in each of the Sectors A through L, at any point in time, for 20,000 years and for the Alternative Sensitivity Case K. For Alternative Sensitivity Case K, a distinction is seen in early time (before 2,000 years), at about 12,000 to 14,000 years, and again past about 19,000 years. During these intervals, Sector B doses remain the highest, but overall, Sector G produces the highest dose at around 16,000 years.

Figure 2.3-6: Mean Dose to a MOP by Sector within 20,000 Years – Alternative Sensitivity Case K

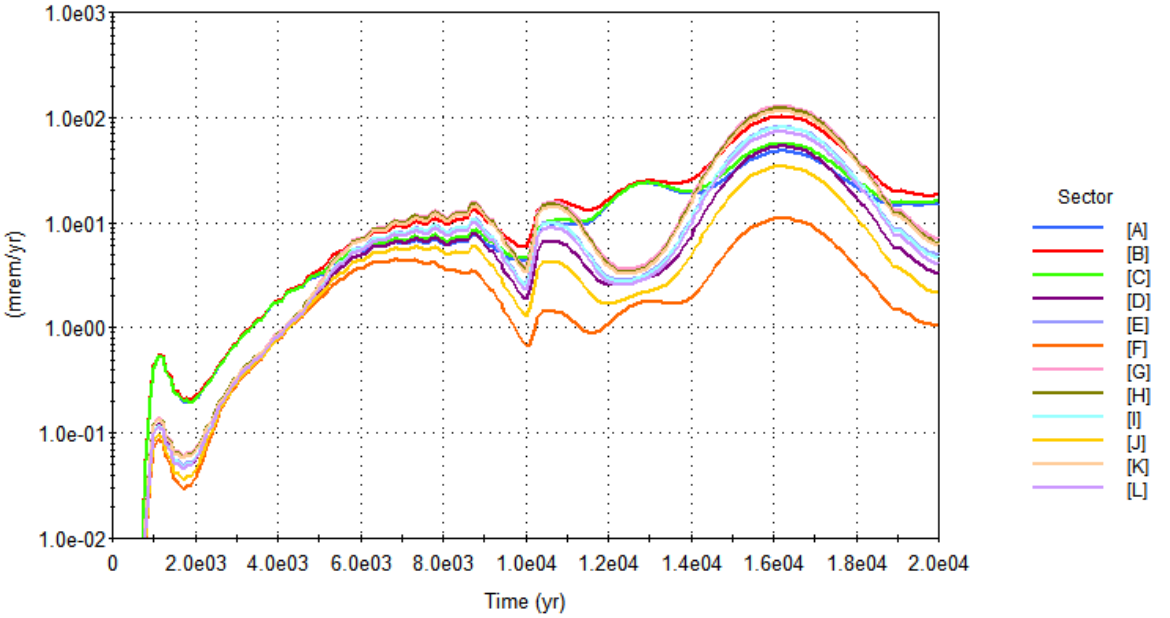

2.3.2 Sensitivity Analysis

Given the uncertainties presented in Section 2.3.2, the next step is to identify those input parameters and other stochastic entities in the model that lead to those uncertainties. Even in complex models, the results are often strongly dependent on only a handful of parameters. What is important for one result (e.g., the I-129 concentration in groundwater) may be insignificant to another, such as the maximum dose to the MOP achieved within 20,000 years. In fact, the maximum dose to the MOP will have different sensitivities at different times, since it is driven by the presence of different radionuclides. For example, a MOP dose may be dominated by Tc-99 at one time and by I-129 at another time, and these doses will be determined by different aspects of the model (different K_ds, dose pathway, consumption rates, radionuclide inventories, etc.). Extracting the important model inputs for results of interest is the subject of the SA.

2.3.2.1 Introduction to SDF Probabilistic Model Sensitivity Analysis

Complex modeling, such as the probabilistic modeling of the SDF, is needed to explore dynamics of systems where multiple variables interact in a nonlinear manner. The probabilistic simulation approach used in the GoldSim model propagates uncertainty regarding the explanatory variables (e.g., inputs such as physical soil properties or inventory mass) through the model to the predicted response (e.g., dose or concentration). Quantitative assessment of the importance of inputs is necessary when the level of uncertainty in the system response exceeds the acceptable threshold specified in the decision-making framework. One of the goals of SA is to identify which variables have distributions that exert the greatest influence on the response.

The SA deals with estimating influence measures for input variables. Influence measures can be estimated in either a qualitative or a quantitative context. A qualitative SA provides a relative ranking of the importance of input factors without incurring the computational cost of quantitatively estimating the percentage of the output variation accounted for by each input factor. For both approaches, the estimates can be obtained either locally or globally within the parameter space. A local SA involves varying one explanatory variable while holding all other explanatory variables constant, and assessing the impact on the model response. This is local in the sense that only a minimal portion of the full explanatory variable space is explored (i.e., the point at which the explanatory variables are held constant). Although local SA is useful in some applications, the region of possible realizations for the model of interest is left largely unexplored. Global SA attempts to explore the possible realizations of the model more completely. The space of possible realizations for the model can be explored using search curves or evaluation of multi-dimensional integrals using *Monte Carlo* methods. However, these approaches to global SA become more computationally intensive as the dimensionality of the model (i.e., the number of model parameters) increases. In this case, the GoldSim SDF model includes over 1,400 stochastic parameters, a rather large dimensionality.

Because of the computational cost, sensitivity analysis of high-dimensional probabilistic models requires efficient algorithms for practical application. In this work, a dataset of 5,000 probabilistic model realizations (e.g., a dataset with 1,400 columns for the stochastic model parameters and one column for a MOP dose as the model response) were analyzed using Gradient Boosting Models (GBM). The GBM analysis provides a global SA that quantifies the importance of explanatory variables using sensitivity indices (SIs), which are metrics based on the explained variance in the response. [ISSN 0885-6125 Vol. 40 No. 2, ISSN 0885-6125 Vol. 24 No. 2] The implementation of GBM used here comes from the *R* statistical package named "gbm" (SDF PA Section 5.6.5.1).

2.3.2.2 Model Fitting and Validation

This section presents detailed discussion of the statistical methods used in the SA. Global sensitivity is estimated here as the proportion of the variance of the response accounted for by each explanatory variable. This estimation is conducted by fitting GBM model predictions to realizations from the GoldSim model. Variance decomposition of the fitted GBM model is then used to estimate SIs. Under this decomposition approach, the goal is to identify the most influential explanatory variables that are identified within a model. The necessary degree of model complexity is assessed using validation metrics, based on comparison of model predictions, with randomly selected subsets of the data. This approach uses the "deviance" of the model as a measure of goodness of fit. The concept of deviance is fundamental to classical statistical hypothesis tests (e.g., the common *t*-test can be derived using a deviance-based framework) and guides the model selection process applied here.

The GBM model fitting approach is based on finding those values of each explanatory variable that result in the greatest difference in mean for the corresponding subsets of the response. For example, if there were only a single explanatory variable, the GBM would identify the value of the explanatory variable that corresponds to a split of the response into two parts. This will ensure that no other split would result in corresponding groups of the

response variable with a greater difference in means. When multiple explanatory variables are present, these multiple splits are referred to as "trees." Each tree results an estimate (e.g., prediction) of the response. As multiple potential trees are evaluated, they are compared to the observed data using a loss function. The selection of the loss function is an influential aspect of the GBM process, and depends on the distribution of the response variable. For data that are sufficiently skewed (e.g., non-normal), the absolute error loss function typically produces more reliable results.

A trade-off exists when considering which loss function to use. The squared-error loss function results in better fitting models, but can do so at the expense of introducing spurious variables into the model selection process when the response distribution is sufficiently skewed. The absolute error loss function produces model predictions with more variability, but is less likely to result in the selection of spurious variables in the model. For this application, the focus has been on using a deviance-based method to obtain models that identify the most important explanatory variables with respect to the observed variability in the response. Therefore, the squared-error function was used in these applications.

Once a GBM model is constructed, each of the explanatory variables that exist in the model can be assigned an SI. The SI is obtained through variance decomposition and can be interpreted as the percentage of variability explained in the model by a given explanatory variable. The sum of the SIs across the entire set of explanatory variables in the model will approximately equal the R^2 of the linear regression of the GoldSim output versus the GBM predictions. The R^2 values for this version of the SDF model indicate the high degree of predictive power of the GBM in fitting the GoldSim model. For the SDF PA Case A endpoints, the R^2 values range from 0.85 to 0.99 with only two less than 0.900 and six greater than 0.950. For the Alternative Sensitivity Case K endpoints, the R^2 values range from 0.90 to 1.0 with only one less than 0.900 and seven greater than 0.950.

In order to assess the relationship between an individual explanatory variable and the response of interest, partial dependence plots are used (these are presented below for each identified endpoint), as shown in Figure 2.3-7. The first panel depicts a density estimate of the simulated response from the GoldSim model. The percentiles of the response distribution in this panel are shaded to provide a context for the partial dependence plots presented in the remaining panels. The colors indicate the percentile range of the response as follows:

1) The 0^{th}-25^{th} percentile region is shaded orange-brown
2) The 25^{th}-50^{th} percentile region is shaded green
3) The 50^{th}-75^{th} percentile region is shaded light blue
4) The 75^{th}-100^{th} percentile region is shaded pink

The y-axis scale of the partial dependence plots is in units of the response distribution (the x-axis of the first panel). Given that each parameter has a different range and strength of influence on the response, the y-axes of the partial dependence panels depict only the range of the response over which a particular parameter is influential. If the original scale of the response were maintained on each partial dependence panel, then the influence of the least influential parameter would not be visible in many cases. To counteract this scale issue, the background of the partial dependence panels is shaded to depict the percentile of the response over which the parameter is influential. For example, if the background of the partial

dependence plot under the partial dependence line is pink, then that indicates the parameter's influence on the upper end of the response distribution (i.e., the 75^{th}-100^{th} percentile of the response).

The partial dependence panels in each figure show the distributions of the explanatory variables (transparent white), and the partial dependence curve (blue line) shows changes in the response as a function of each explanatory variable. In the example provided (Figure 2.3-7), the variable has a normal input distribution, and the dependence of the result on this parameter spans nearly the entire range of the variable, with a flat (unresponsive) part at the upper end.

The partial dependence is determined through the integration across the joint density to obtain a marginal distribution. The integration is performed using a "weighted tree traversal" measure that is analogous more common than integration procedures performed with Riemann or Lebesgue measures. The vertical axis of the partial dependence plot shows the change in the response variable as a function of the changes in the explanatory variable.

With standard linear regression techniques, it is assumed that the relationship between the response and the explanatory variable is a constant (e.g., the parameter estimates in the linear model). With the GBM approach, this relationship is not constrained by assumptions of linearity, and the partial dependence plots show the database estimate of the relationship between the response and the explanatory variable. This is useful for understanding the influence of changes in a single explanatory variable, when integrating across all other explanatory variables.

Figure 2.3-7: Example of a Result Probability Density and Partial Dependence Plot

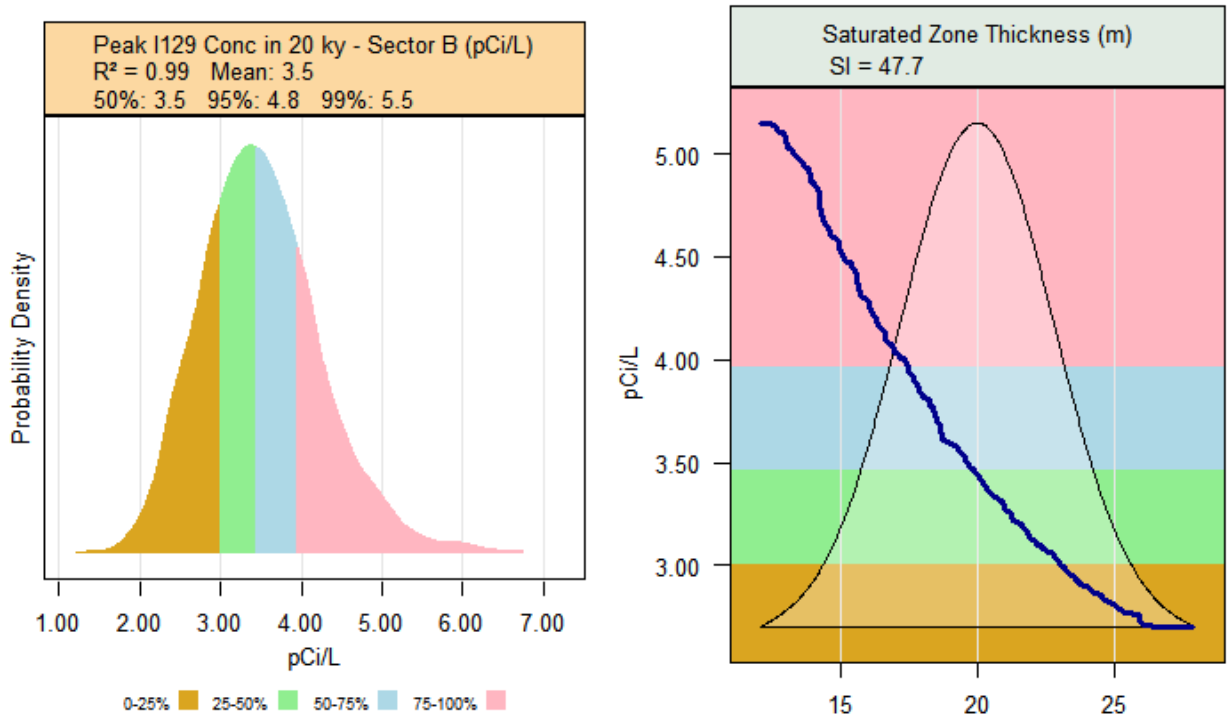

2.3.2.3 Summary Statistics for Endpoints

Exporting model results follows the simple procedure outlined in the SDF GoldSim model, in the containers, *SensitivityAnalysis_Old* (for SDF PA Case A) and *SensitivityAnalysis_New* (for Alternative Sensitivity Case K). The tabulated raw data contents of the element *Endpoints_Old_1* (for SDF PA Case A) and *Endpoints_New_1* (for Alternative Sensitivity Case K) are exported to a tab-delimited text file. Since each individual model run consists of only 1,000 realizations, five runs with different Latin Hypercube seed values were combined to get 5,000 different realizations. This was done for both Cases A and K. The different seed values cause a different (though statistically similar) set of 1,000 parameter values to be run.

For each endpoint, as shown in Tables 2.3-3 and 2.3-4, the most significant parameters identified by the SA are presented, along with the R^2 and SI for each. Following Tables 2.3-3 and 2.3-4, in Section 2.3.3.4 (SDF PA Case A) and 2.3.3.5 (Alternative Sensitivity Case K) are a series of figures showing the partial dependence of each of the highest SIs for each endpoint. The SIs less than 5.0 are not reported.

Table 2.3-3: Most Sensitive Parameters for Endpoints of Interest – SDF PA Case A

Endpoint	R^2	SI Rank	Input Parameter	SI
Maximum dose to MOP at any Sector within 10,000 years (mrem/yr)	0.92	1	saturated zone thickness	17.8
		2	fraction of vegetables grown locally	17.6
		3	K_d for radium in sandy soil	17.0
		4	vegetable production yield	13.1
		5	water ingestion rate	12.1
Maximum dose to MOP at any Sector within 20,000 years (mrem/yr)	0.85	1	fraction of vegetables grown locally	17.7
		2	saturated zone thickness	17.4
		3	vegetable production yield	14.4
		4	water ingestion rate	12.2
		5	pore volumes to Region III oxidized concrete	10.9
Maximum dose to MOP at Sector B within 10,000 years (mrem/yr)	0.92	1	saturated zone thickness	17.8
		2	fraction of vegetables grown locally	17.7
		3	K_d for radium in sandy soil	17.0
		4	vegetable production yield	13.1
		5	water ingestion rate	12.1
Maximum dose to MOP at Sector B within 20,000 years (mrem/yr)	0.85	1	fraction of vegetables grown locally	17.7
		2	saturated zone thickness	17.4
		3	vegetable production yield	14.5
		4	water ingestion rate	12.2
		5	pore volumes to Region III oxidized concrete	10.9
Maximum dose to MOP at Sector J within 10,000 years(mrem/yr)	0.97	1	fish ingestion rate	68.6
		2	saturated zone thickness	14.6
		3	K_d for radium in sandy soil	9.61
Maximum dose to MOP at Sector J within 20,000 years (mrem/yr)	0.94	1	fish ingestion rate	68.2
		2	saturated zone thickness	18.6
		3	K_d for Radium in sandy soil	5.43
Maximum conc. of Tc-99 at Sector B within 20,000 years (pCi/L)	0.97	1	pore volumes to Region III oxidized concrete	55.50
		2	pore volumes to Region II oxidized concrete	21.6
		3	saturated zone thickness	7.96
		4	K_d for technetium in Region II reducing concrete	7.09
Maximum conc. of Tc-99 at Sector J within 20,000 years (pCi/L)	0.98	1	K_d for technetium in Region II reducing concrete	43.7
		2	pore volumes to Region III oxidized concrete	29.5
		3	pore volumes to Region II oxidized concrete	14.7
		4	saturated zone thickness	7.34
Maximum conc. of I-129 at Sector B within 20,000 years (pCi/L)	0.99	1	saturated zone thickness	47.7
		2	K_d for iodine in Region II reducing concrete	29.2
		3	I-129 waste tank inventory uncertainty – FDCs	21.4

conc. = concentration

Table 2.3-3: Most Sensitive Parameters for Endpoints of Interest – SDF PA Case A (Continued)

Endpoint	R^2	SI Rank	Input Parameter	Sensitivity Index
Maximum conc. of I-129 at Sector J within 20,000 years (pCi/L)	0.99	1	saturated zone thickness	47.7
		2	K_d for iodine in Region II reducing concrete	27.8
		3	I-129 waste tank inventory uncertainty – FDCs	22.6
Maximum conc of Ra-226 at Sector B within 20,000 years (pCi/L)	0.94	1	K_d for radium in sandy soil	40.2
		2	saturated zone thickness	37.5
		3	Th-230 waste tank inventory uncertainty – Vault 4	6.30
Maximum conc of Ra-226 at Sector J within 20,000 years (pCi/L)	0.98	1	K_d for radium in sandy soil	70.9
		2	saturated zone thickness	16.8
		3	unsaturated zone thickness – FDCs	6.03

conc. = concentration

Table 2.3-4: Most Sensitive Parameters for Endpoints of Interest – Alternative Sensitivity Case K

Endpoint	R^2	SI Rank	Input Parameter	Sensitivity Index
Maximum dose to MOP at any Sector within 10,000 years (mrem/year)	0.90	1	water ingestion rate	31.5
		2	saturated zone thickness	22.4
		3	I-129 waste tank inventory uncertainty – FDCs	10.1
		4	pore volumes to Region II oxidized concrete	8.10
		5	pore volumes to Region III oxidized concrete	6.62
Maximum dose to MOP at any Sector within 20,000 years (mrem/ year)	0.94	1	fraction of vegetables grown locally	25.1
		2	saturated zone thickness	20.9
		3	water ingestion rate	16.1
		4	garden till depth	12.7
		5	non-leafy vegetable ingestion rate	10.1
Maximum dose to MOP at Sector B within 10,000 years (mrem/ year)	0.87	1	water ingestion rate	27.6
		2	saturated zone thickness	21.9
		3	fish ingestion rate	8.84
		4	I-129 waste tank inventory uncertainty – FDCs	8.83
		5	pore volumes to Region II oxidized concrete	6.57
Maximum dose to MOP at Sector B within 20,000 years (mrem/year)	0.92	1	fraction of vegetables grown locally	23.7
		2	saturated zone thickness	21.9
		3	water ingestion rate	16.9
		4	garden till depth	11.3
		5	non-leafy vegetable ingestion rate	9.47
Maximum dose to MOP at Sector G within 10,000 years (mrem/ year)	0.90	1	water ingestion rate	31.3
		2	saturated zone thickness	22.4
		3	I-129 waste tank inventory uncertainty – FDCs	10.1
		4	pore volumes to Region II oxidized concrete	8.14
		5	pore volumes to Region III oxidized concrete	6.94
Maximum dose to MOP at Sector G within 20,000 years (mrem/year)	0.94	1	fraction of vegetables grown locally	25.2
		2	saturated zone thickness	20.8
		3	water ingestion rate	16.3
		4	garden till depth	12.7
		5	non-leafy vegetable ingestion rate	10.1
Maximum conc. of Tc-99 at Sector B within 20,000 years (pCi/L)	1.0	1	saturated zone thickness	68.9
		2	Tc-99 waste tank inventory uncertainty – FDCs	30.9
Maximum conc. of Tc-99 at Sector G within 20,000 years (pCi/L)	1.0	1	saturated zone thickness	69.3
		2	Tc-99 waste tank inventory uncertainty – FDCs	30.6

conc. = concentration

Table 2.3-4: Most Sensitive Parameters for Endpoints of Interest – Alternative Sensitivity Case K (Continued)

Endpoint	R^2	SI Rank	Input Parameter	Sensitivity Index
Maximum conc. of I-129 at Sector B within 20,000 years (pCi/L)	0.96	1	saturated zone thickness	41.5
		2	I-129 waste tank inventory uncertainty – FDCs	20.3
		3	pore volumes to Region II oxidized concrete	17.6
		4	pore volumes to Region III oxidized concrete	17.3
Maximum conc. of I-129 at Sector G within 20,000 years (pCi/L)	0.96	1	saturated zone thickness	42.1
		2	I-129 waste tank inventory uncertainty – FDCs	20.0
		3	pore volumes to Region II oxidized concrete	17.4
		4	pore volumes to Region III oxidized concrete	17.1
Maximum conc of Ra-226 at Sector B within 20,000 years (pCi/L)	0.97	1	K_d for radium in sandy soil	81.2
		2	saturated zone thickness	10.2
Maximum conc of Ra-226 at Sector G within 20,000 years (pCi/L)	1.0	1	K_d for radium in sandy soil	86.2
		2	saturated zone thickness	6.97
Maximum conc of Cs-135 along streamline within 20,000 years (pCi/L)	0.97	1	saturated zone thickness	39.7
		2	K_d for cesium in Region II reducing saltstone	22.6
		3	K_d for cesium in Region II reducing floor concrete	18.9
		4	Cs-135 waste tank inventory uncertainty – Vault 4	16.3

conc. = concentration

2.3.2.4 SDF PA Case A Partial Dependence Plots

The partial dependence plots for SDF PA Case A are shown in the figures within this section. These plots identify the model input parameters that are most significant in determining the model endpoints identified in Table 2.3-3.

In the case of the peak dose (the maximum achieved through time) to a MOP at any of the sectors within 10,000 years, and assuming SDF PA Case A (Figure 2.3-8), the five most influential variables are remarkably even in sensitivity, all describing between 10 % and 20 % of the total variation in the endpoint. They are, in order of importance, the thickness of the saturated zone, the fraction of consumed vegetables that are grown in a local garden; the K_d for radium in sandy soil, the vegetable garden productivity (mass of vegetables produced per unit area of garden), and the receptor's drinking water consumption rate.

Note that the dose increases with the fraction of locally grown vegetables, which is to be expected, and the dose decreases with the higher vegetable production yield. This trend reflects the decrease in radionuclide mass up-take per unit mass of vegetables produced caused by the increased mass of vegetables produced.

Figure 2.3-8: Probability Density and Partial Dependence of Peak MOP Dose, Any Sector within 10,000 Years – SDF PA Case A

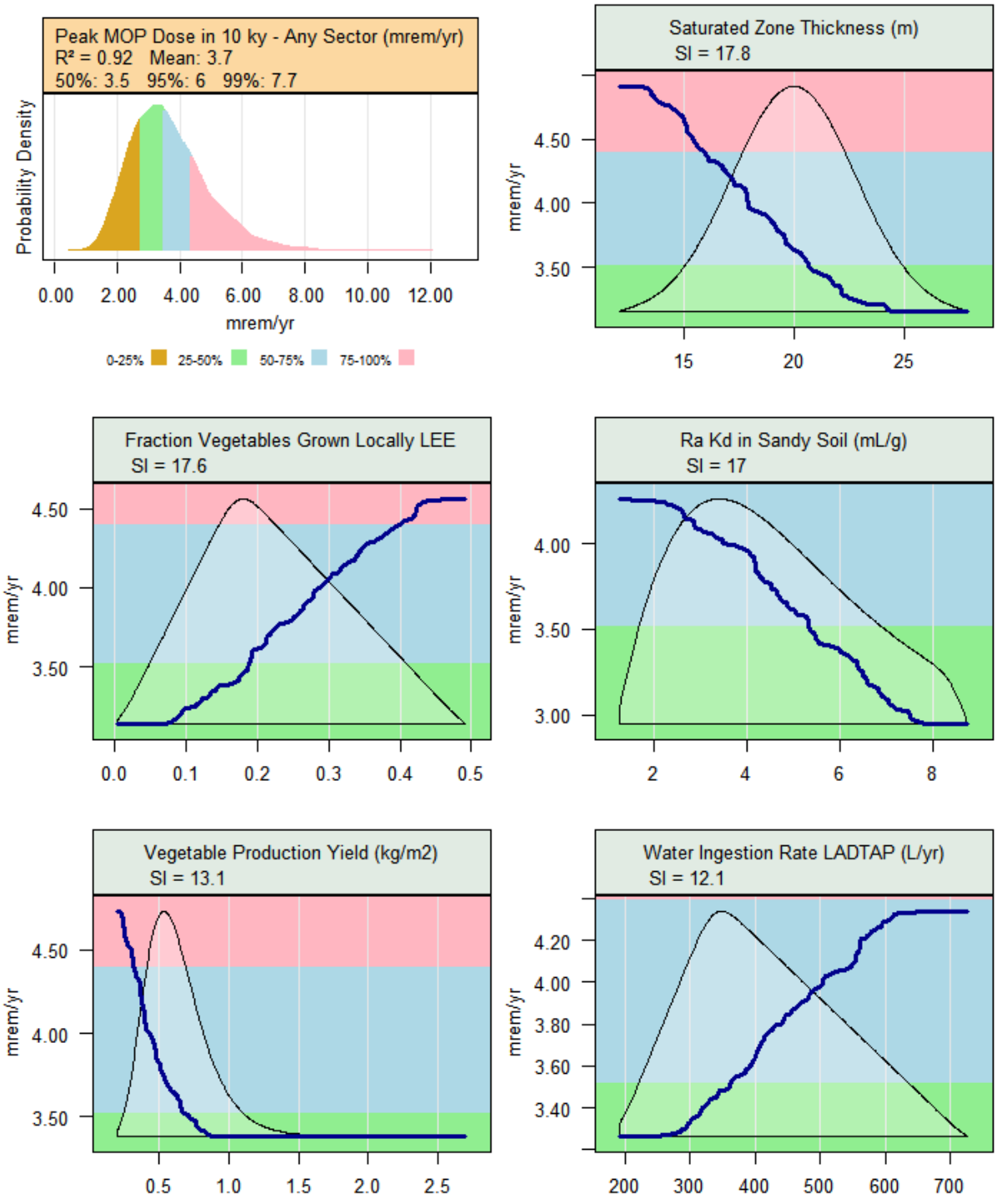

Figure 2.3-9 shows the SI plots for the same dose to a MOP at any sector, for SDF PA Case A, but for the peak dose within 20,000 years. This shows most of the same variables as for the 10,000-year peak, with the addition of the number of pore volumes of water flowing through concrete that are needed to chemically change the concrete from oxidized Region II to oxidized Region III.

Figure 2.3-9: Probability Density and Partial Dependence of Peak MOP Dose, Any Sector within 20,000 Years – SDF PA Case A

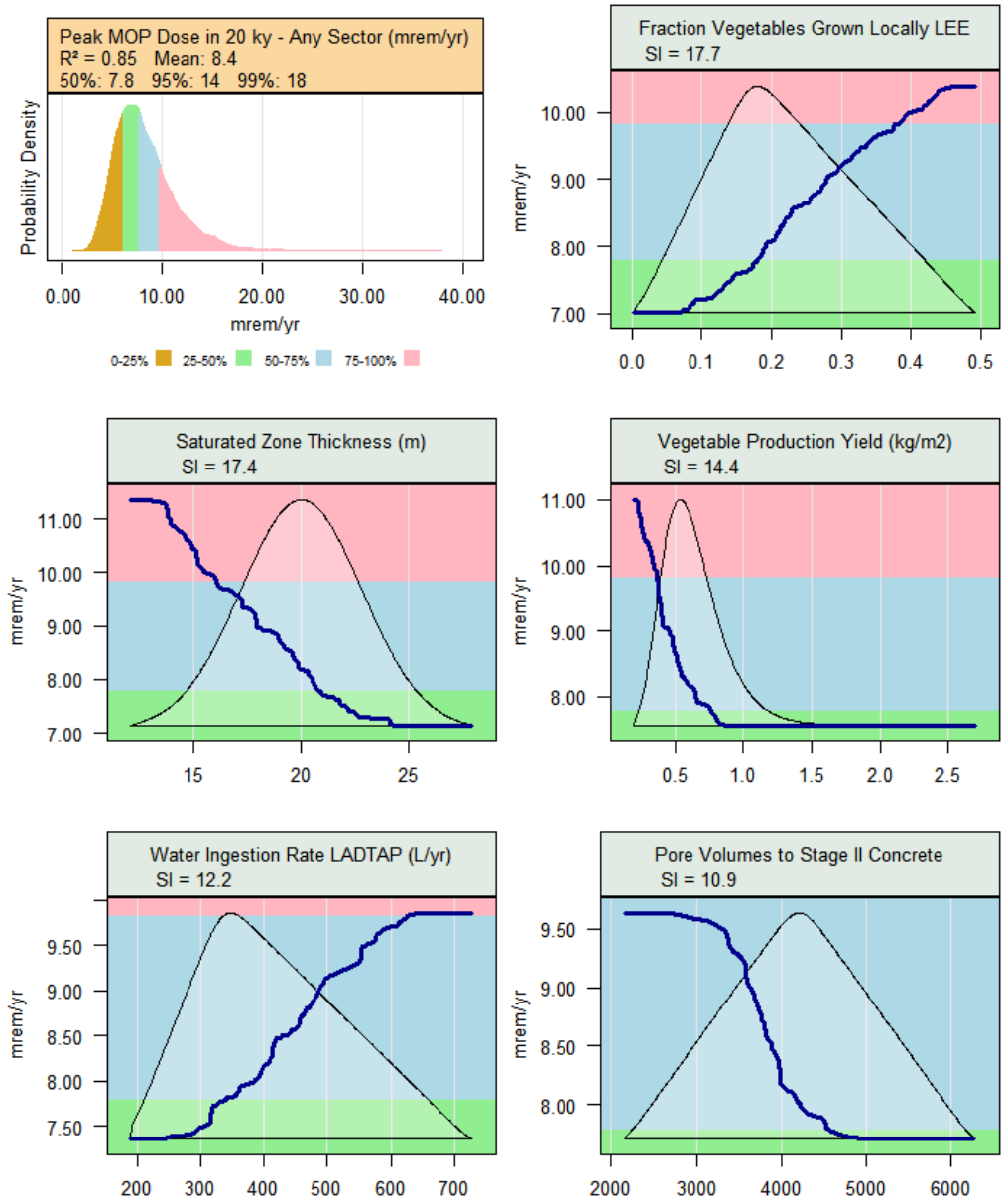

Note: "Pore Volumes to Stage II Concrete" is the number of pore volumes required for concrete to transition from oxidized Region II to oxidized Region III.

The SA results for the 10,000-year peak MOP dose within Sector B (Figure 2.3-10) shows that Sector B is the most significant sector driving the dose within 10,000 years for SDF PA Case A, since it essentially duplicates the sensitivity of peak dose for all sectors within 10,000 years (see Figure 2.3-8). The same sensitive variables are identified.

Figure 2.3-10: Probability Density and Partial Dependence of Peak MOP Dose, Sector B within 10,000 Years – SDF PA Case A

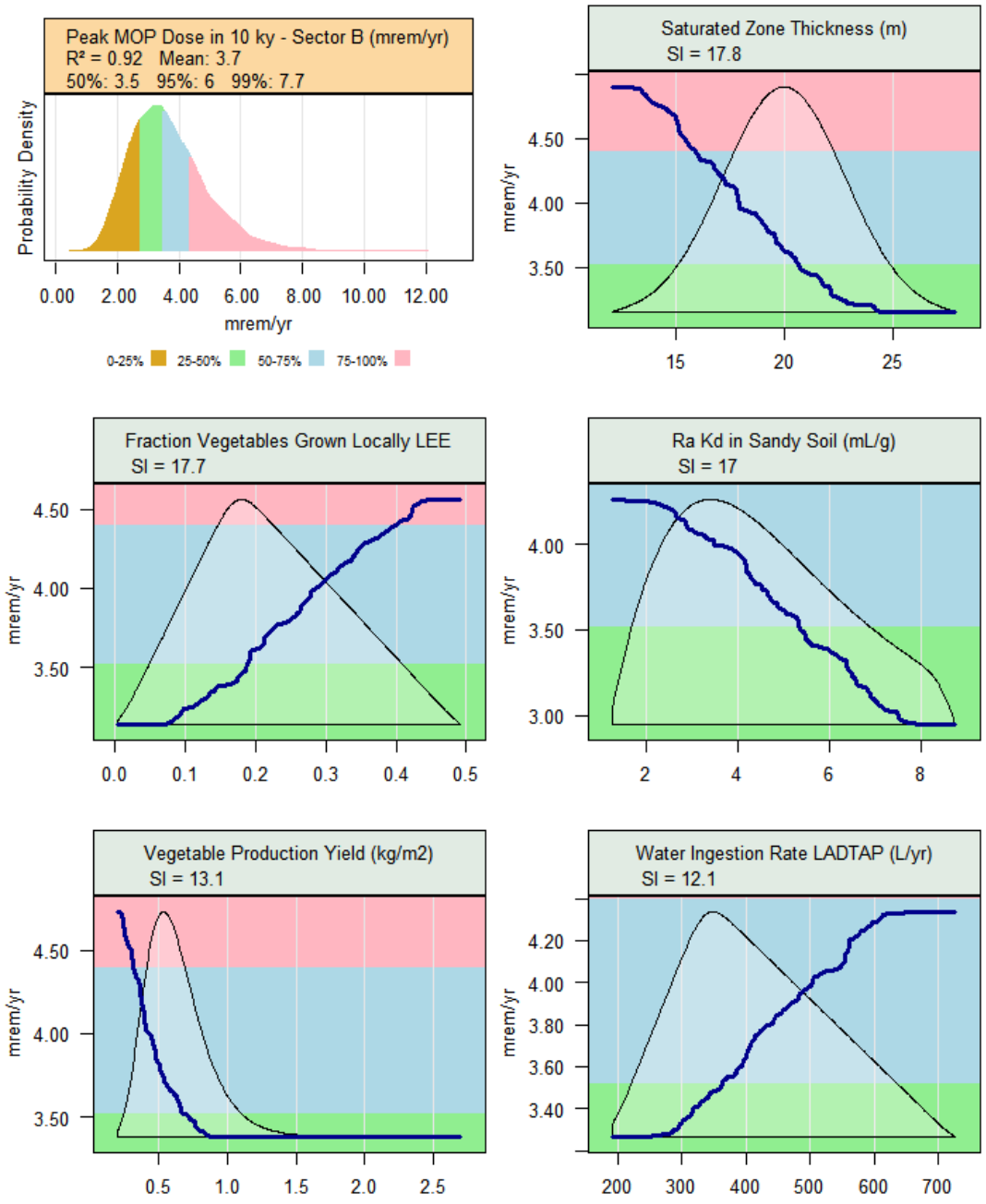

The sensitivities for peak MOP dose within 20,000 years in Sector B (Figure 2.3-11) are likewise essentially identical to those of the 20,000-year peak dose for any sector (Figure 2.3-9). Again, this is because Sector B has the highest dose of any sector for SDF PA Case A.

Figure 2.3-11: Probability Density and Partial Dependence of Peak MOP Dose, Sector B within 20,000 Years – SDF PA Case A

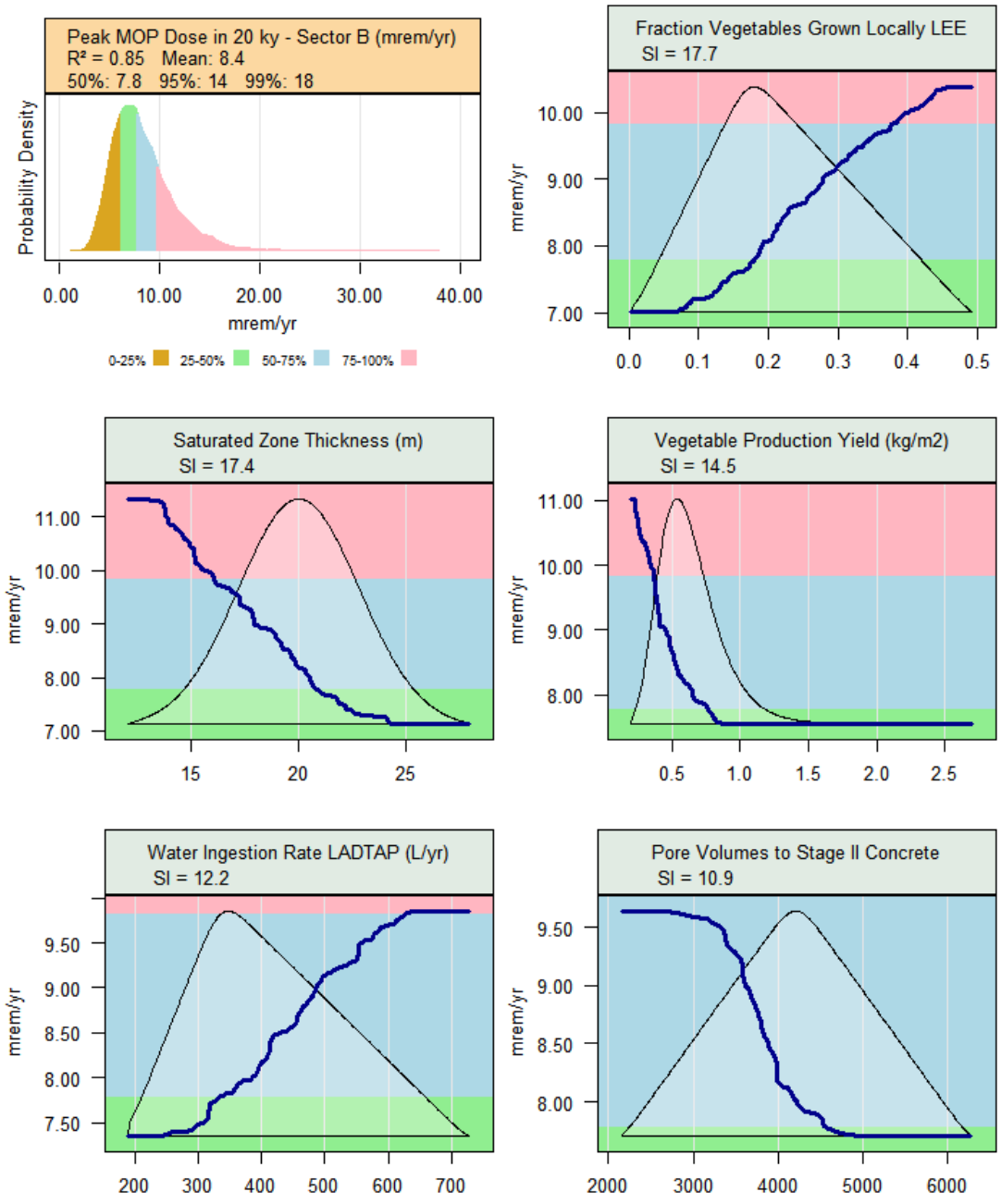

Note: "Pore Volumes to Stage II Concrete" is the number of pore volumes required for concrete to transition from oxidized Region II to oxidized Region III.

The peak 10,000-year MOP dose within Sector J is driven overwhelmingly by the receptor's consumption of fish, as seen in Figure 2.3-12. Following that is the saturated zone thickness and the K_d for radium in sandy soil. The fish consumption pathway assumes that fish are caught from a local stream or river in the sector with the highest radionuclide concentration.

Figure 2.3-12: Probability Density and Partial Dependence of Peak MOP Dose, Sector J within 10,000 Years – SDF PA Case A

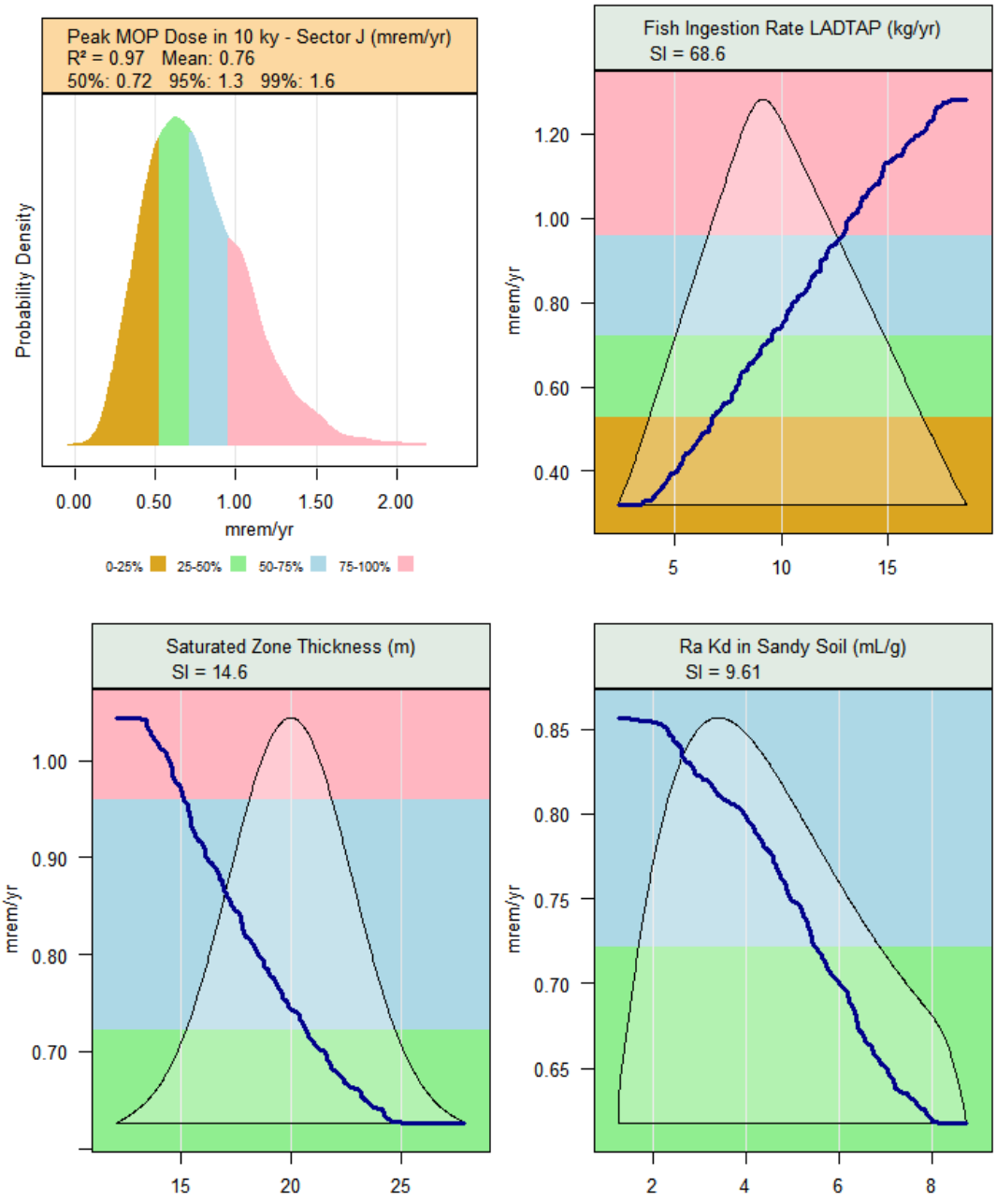

Similar to results in Sector J at 10,000 years, the peak MOP dose within 20,000 years is dominated by the same three parameters (see Figure 2.3-13).

Figure 2.3-13: Probability Density and Partial Dependence of Peak MOP Dose, Sector J within 20,000 Years – SDF PA Case A

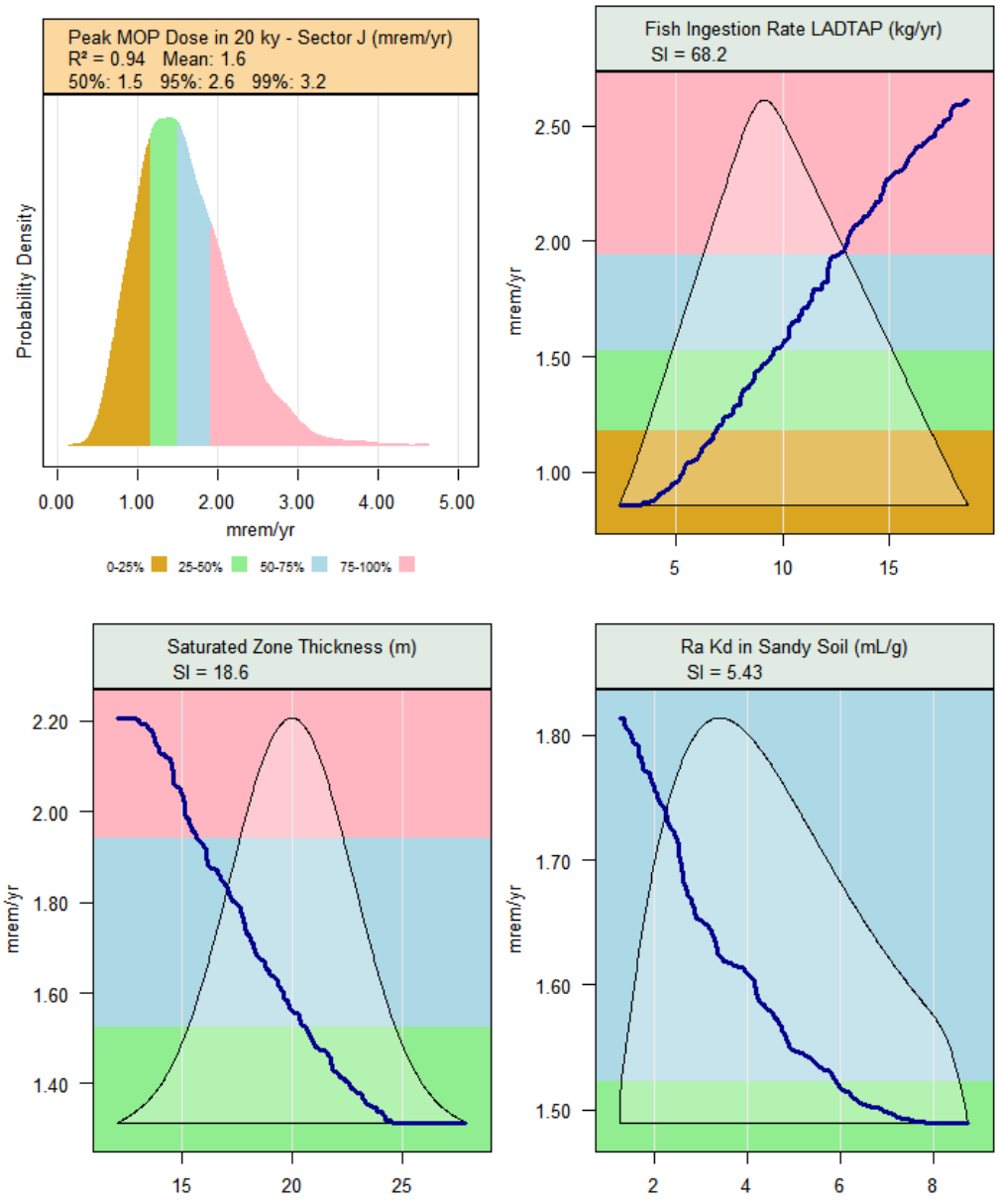

The SA is also used to examine radionuclide concentrations in groundwater at the location where a receptor might obtain water from a well. Figure 2.3-14 shows that the 20,000-year peak concentration of Tc-99 at Sector B is driven largely by the number of pore volumes of water needed to transition from oxidized Region II concrete to oxidized Region III concrete. Secondary to this parameter is the number of pore volumes to transition from reducing Region II and oxidized Region II, the saturated zone thickness, and the K_d of technetium in

reducing Region II concrete. Clearly, the aging of concrete and its associated changes in technetium K_d are highly significant to the transport of Tc-99.

Figure 2.3-14: Probability Density and Partial Dependence of Peak Concentration of Tc-99 at Sector B within 20,000 Years – SDF PA Case A

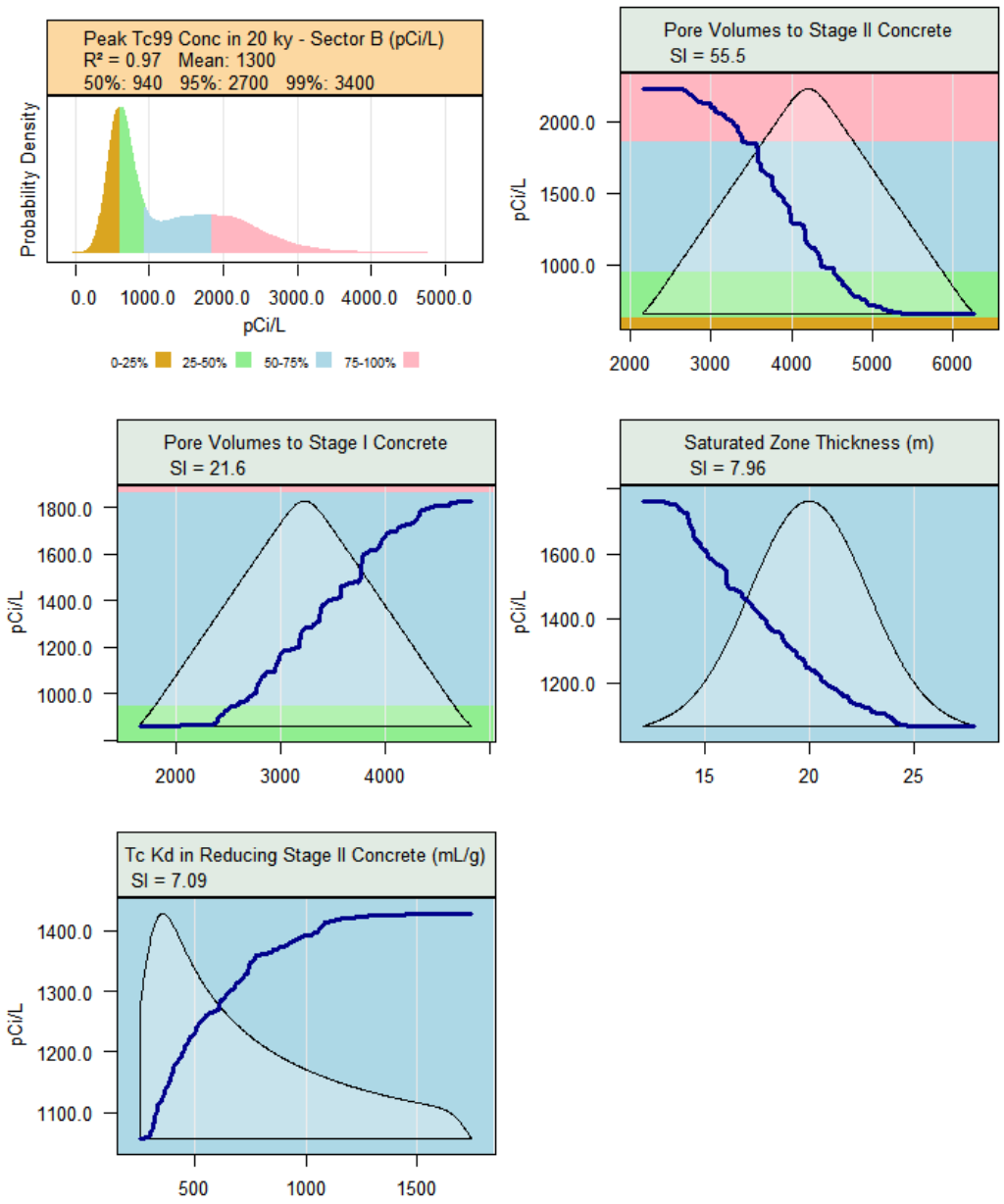

Note: "Pore Volumes to Stage II Concrete" is the number of pore volumes required for concrete to transition from oxidized Region II to oxidized Region III. "Pore Volumes to Stage I Concrete" is the number of pore volumes required for concrete to transition from reducing Region II to oxidized Region II. "Tc Kd in Reducing Stage II Concrete" is the K_d value for technetium in reducing Region II concrete.

Figure 2.3-15 shows the 20,000-year peak Tc-99 concentration at Sector J, which is driven by the same variables as the 10,000-year peak concentration, though with a different ranking of significance.

Figure 2.3-15: Probability Density and Partial Dependence of Peak Concentration of Tc-99 at Sector J within 20,000 Years – SDF PA Case A

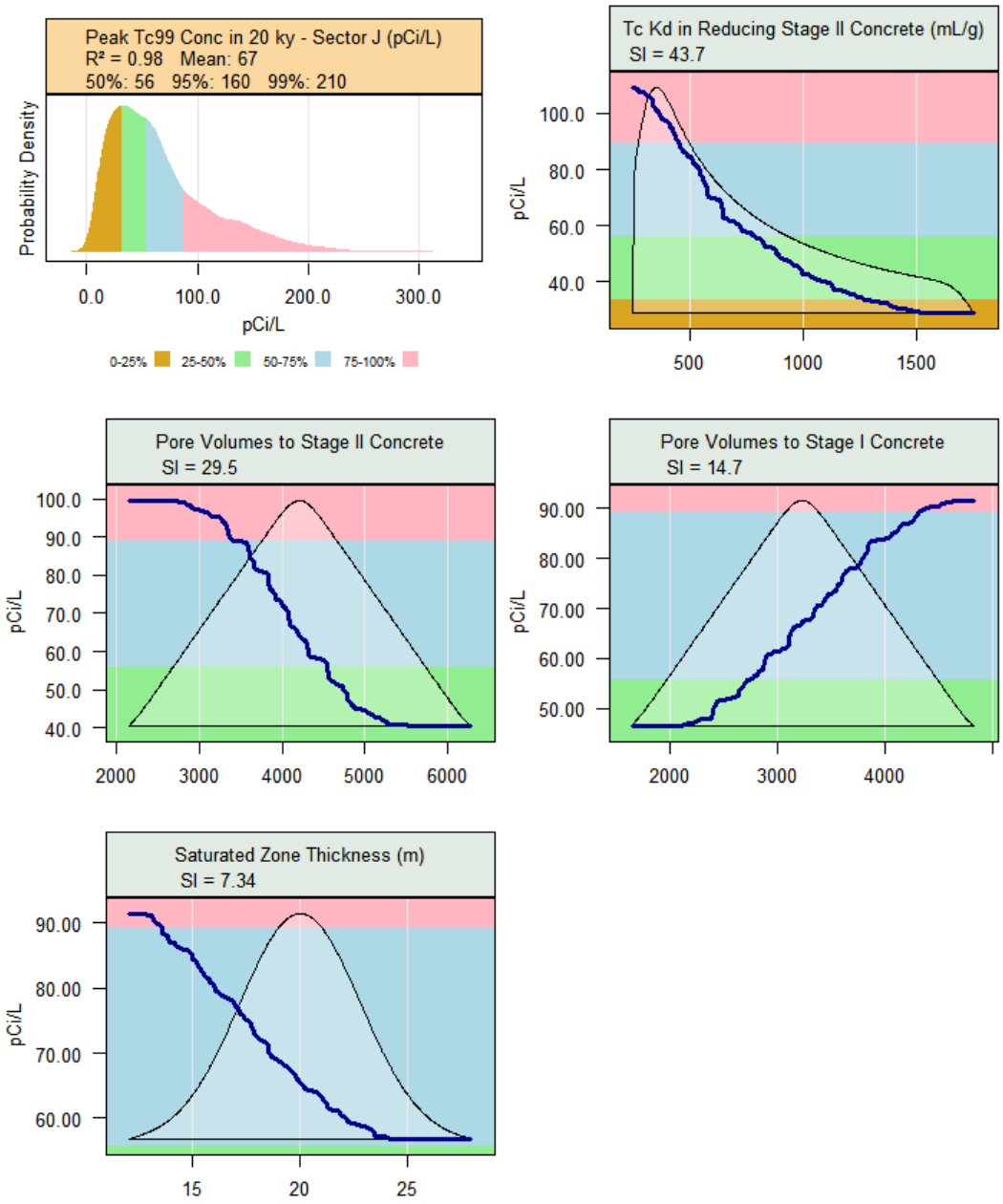

Note: "Tc Kd in Reducing Stage II Concrete" is the K_d value for technetium in reducing Region II concrete. "Pore Volumes to Stage II Concrete" is the number of pore volumes required for concrete to transition from oxidized Region II to oxidized Region III. "Pore Volumes to Stage I Concrete" is the number of pore volumes required for concrete to transition from reducing Region II to oxidized Region II.

Similar to Tc-99, the 20,000-year maximum groundwater concentrations for I-129 are driven by the saturated zone thickness and the reducing stage II concrete K_d, as seen in Figure 2.3-16. The third most important variable is the inventory uncertainty parameter for I-129 in the FDCs.

Figure 2.3-16: Probability Density and Partial Dependence of Peak Concentration of I-129 at Sector B within 20,000 Years – SDF PA Case A

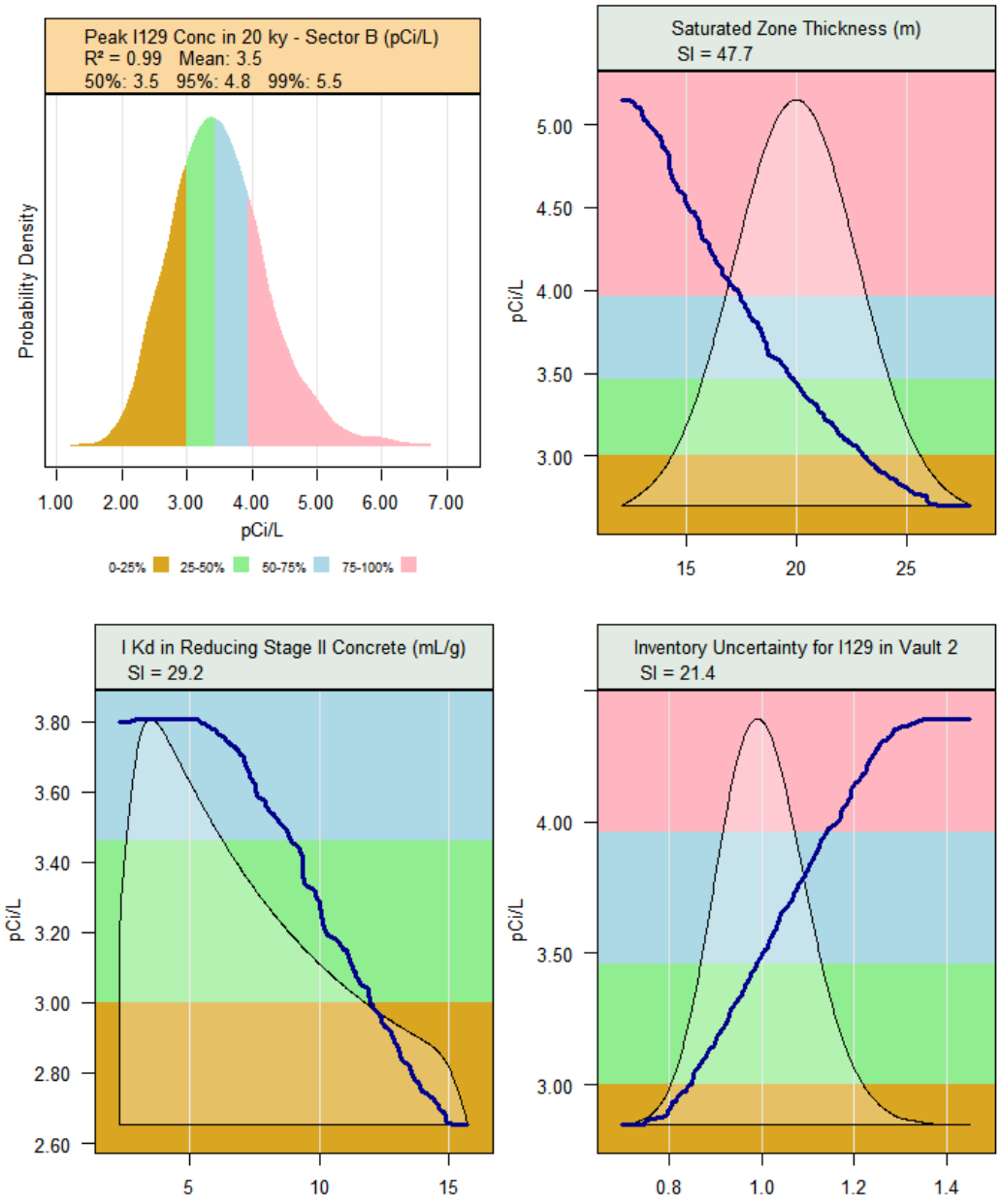

Note: "I Kd in Reducing Stage II Concrete" is the K_d value for iodine in reducing Region II concrete.

As seen in Figure 2.3-17, the 20,000-year peak concentration of I-129 at Sector J is driven by the same variables that are identified as significant for the I-129 peak at Sector B, and with the same degree of influence.

Figure 2.3-17: Probability Density and Partial Dependence of Peak Concentration of I-129 at Sector J within 20,000 Years – SDF PA Case A

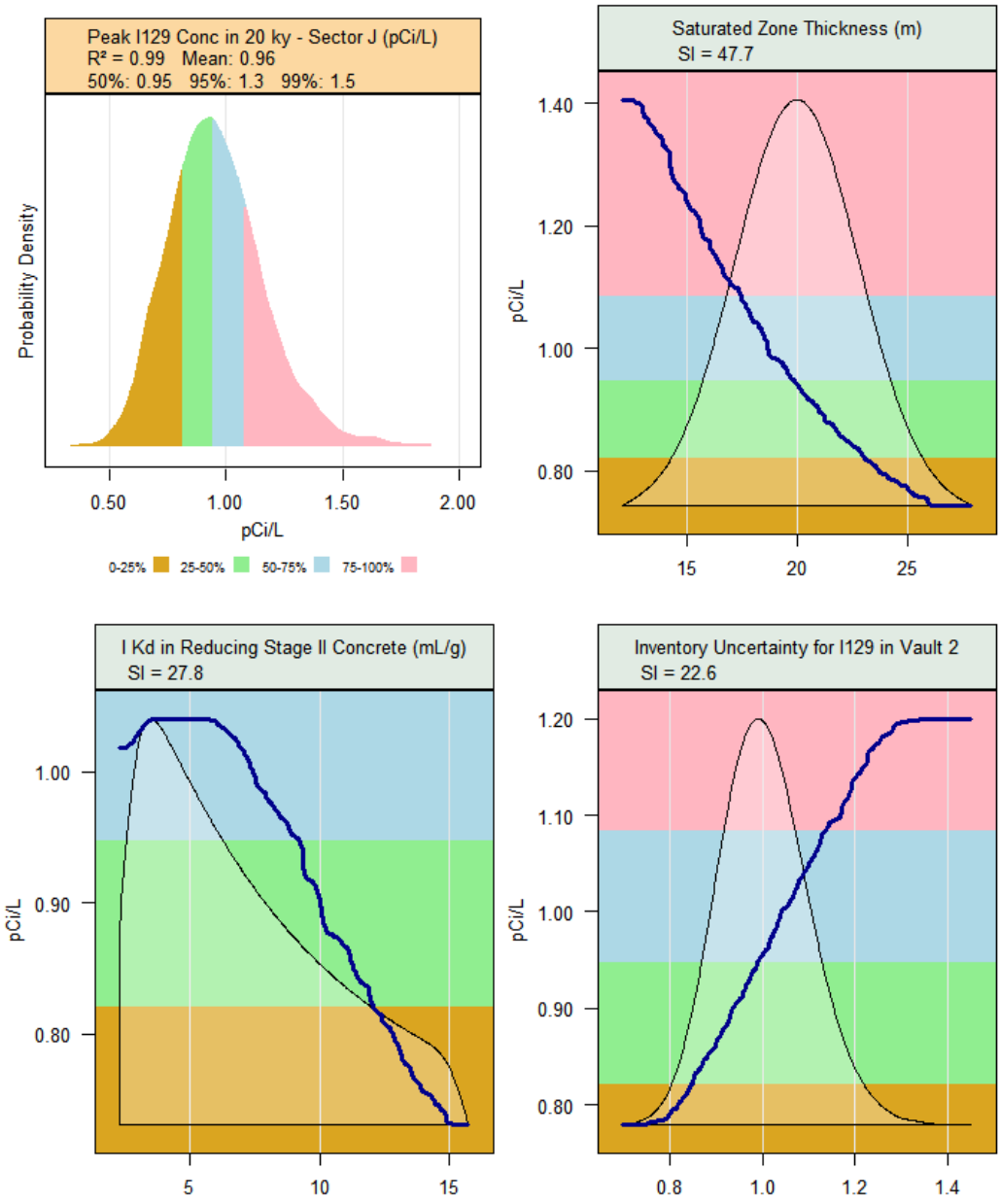

Note: "I Kd in Reducing Stage II Concrete" is the K_d value for iodine in reducing Region II concrete.

The 20,000-year peak concentration of Ra-226 at Sector B is driven by the K_d for radium in sandy soils and the saturated zone thickness (Figure 2.3-18) to nearly the same degree. Minor significance is attributable to the waste inventory of the Th-230 disposed in Vault 4. The immediate parent of Ra-226 is Th-230.

Figure 2.3-18: Probability Density and Partial Dependence of Peak Concentration of Ra-226 at Sector B within 20,000 Years – SDF PA Case A

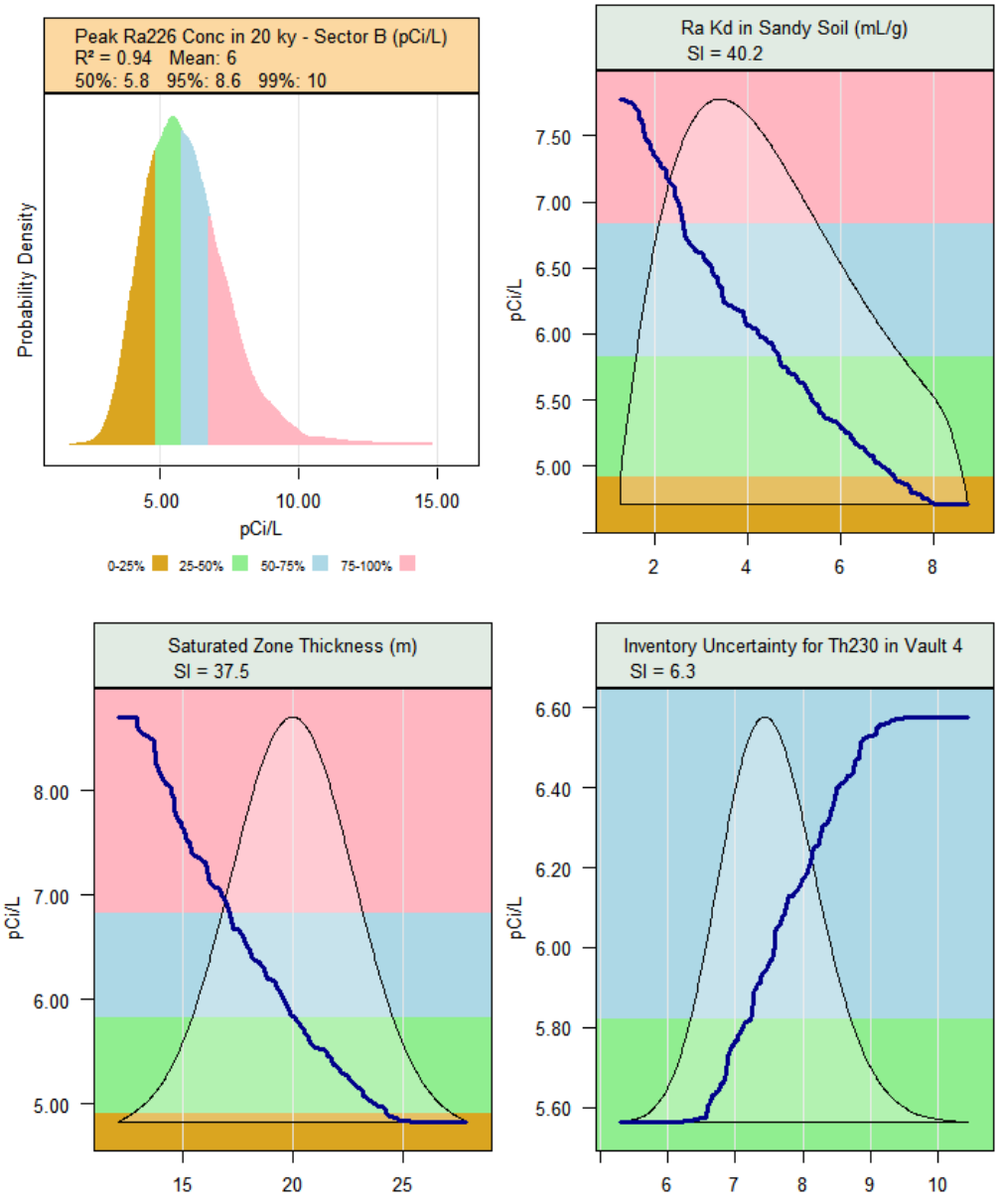

The 20,000-year peak concentration of Ra-226 at Sector J (Figure 2.3-19) is dominated by the K_d for radium in sandy soils, with the saturated zone thickness playing a lesser role. The unsaturated zone thickness has a minor, narrower influence below the FDCs.

Figure 2.3-19: Probability Density and Partial Dependence of Peak Concentration of Ra-226 at Sector J within 20,000 Years – SDF PA Case A

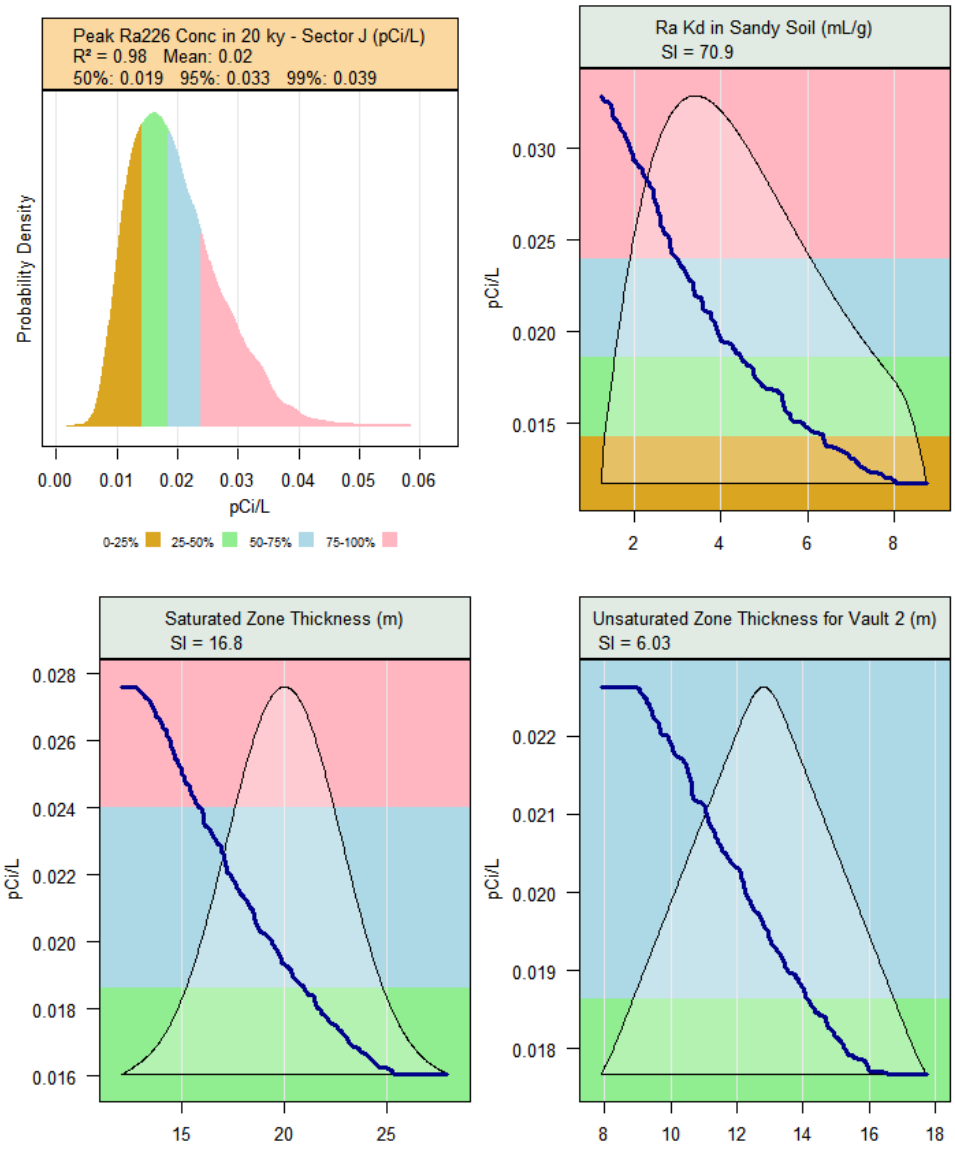

2.3.3.5 Alternative Sensitivity Case K Partial Dependence Plots

The partial dependence plots for Alternative Sensitivity Case K are shown in the figures within this section. The partial dependence plots identify the model input parameters that are most significant in determining the model endpoints identified in Table 2.3-2. Summaries of significant variables are presented in Table 2.3-4.

Figure 2.3-20 shows that for Alternative Sensitivity Case K, the variation in the 10,000-year peak dose to a MOP in any sector is primarily due to the receptor's rate of water consumption and the thickness of the saturated zone. Of lesser influence is the inventory uncertainty parameter for I-129 in the FDCs, and the number of pore volumes of water to

transition concrete from reducing Region II to oxidizing Region II and from oxidizing Region II to oxidizing Region III.

Figure 2.3-20: Probability Density and Partial Dependence of Peak MOP Dose, Any Sector within 10,000 Years – Alternative Sensitivity Case K

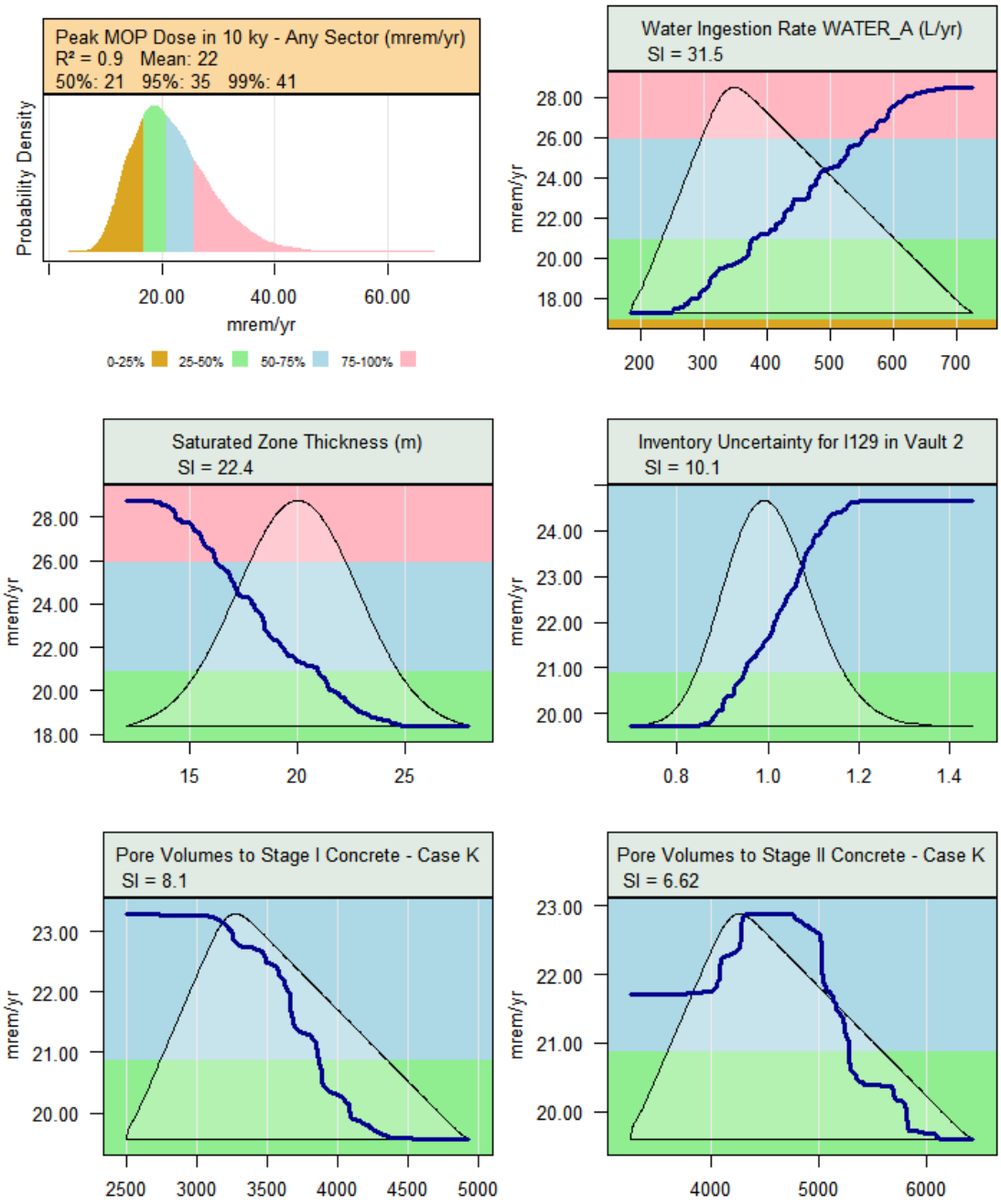

Note: "Pore Volumes to Stage I Concrete" is the number of pore volumes required for concrete to transition from reducing Region II to oxidized Region II. "Pore Volumes to Stage II Concrete" is the number of pore volumes required for concrete to transition from oxidized Region II to oxidized Region III.

For the 20,000-year peak MOP dose at any sector for Alternative Sensitivity Case K (Figure 2.3-21), there are five variables with SIs above 5.0: the fraction of vegetables grown locally, the saturated zone thickness, the receptor's drinking water ingestion rate, the till (mixing) depth of the garden, and the receptor's ingestion rate of non-leafy vegetables.

Figure 2.3-21: Probability Density and Partial Dependence of Peak MOP Dose, Any Sector within 20,000 Years – Alternative Sensitivity Case K

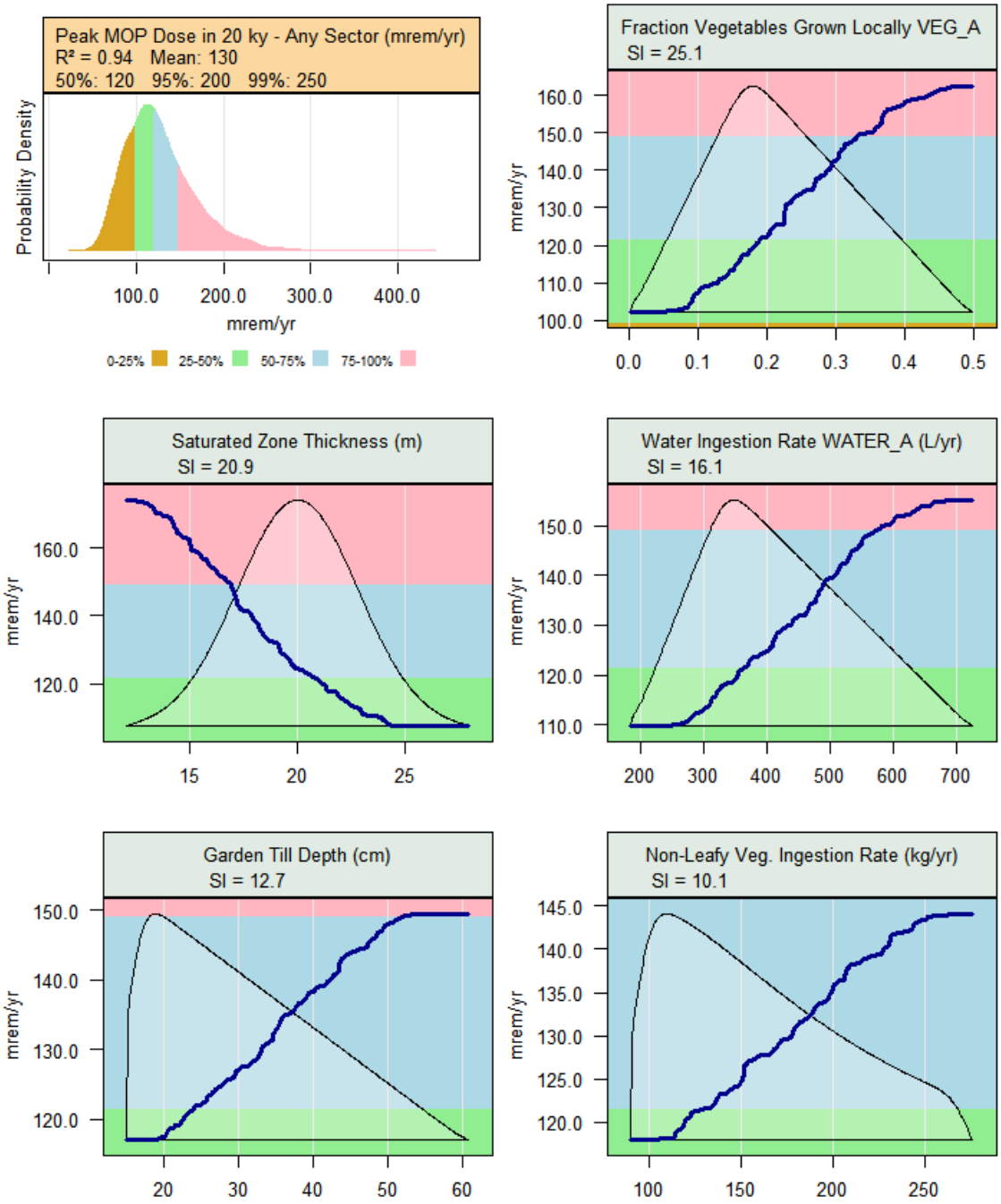

The peak 10,000-year MOP dose within Sector B for Alternative Sensitivity Case K (Figure 2.3-22) has four of the five significant variables that are the same as those for the peak MOP dose at any sector (Figure 2.3-20). The receptor's fish ingestion rate is also a sensitive parameter.

Figure 2.3-22: Probability Density and Partial Dependence of Peak MOP Dose, Sector B within 10,000 Years – Alternative Sensitivity Case K

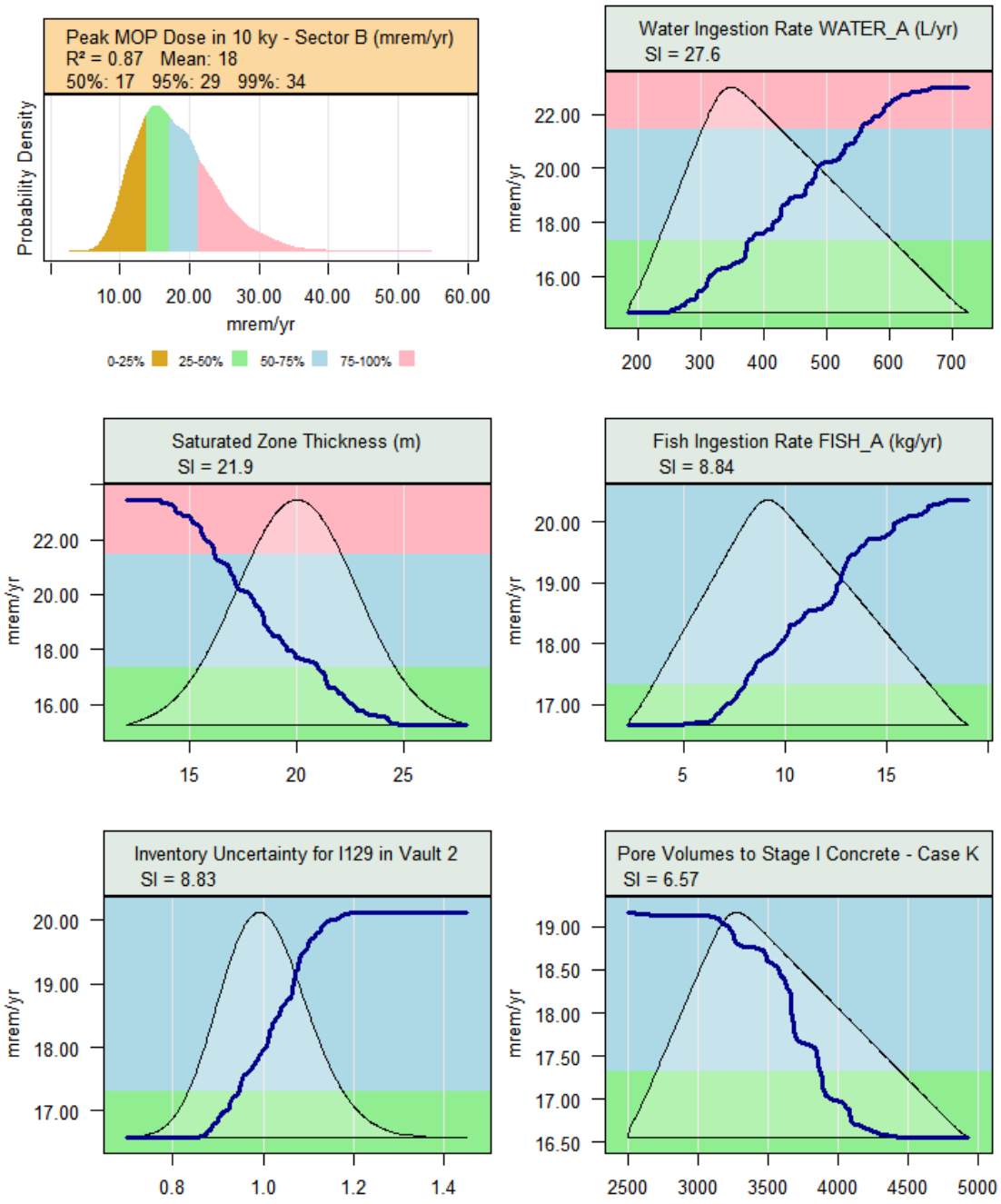

Note: "Pore Volumes to Stage I Concrete" is the number of pore volumes required for concrete to transition from reducing Region II to oxidized Region II.

The endpoint for the 20,000-year peak dose (Figure 2.3-23) for Sector B identifies the same five variables with SIs above 5.0 as those found for any sector within 20,000 years (Figure 2.3-21).

Figure 2.3-23: Probability Density and Partial Dependence of Peak MOP Dose, Sector B within 20,000 Years – Alternative Sensitivity Case K

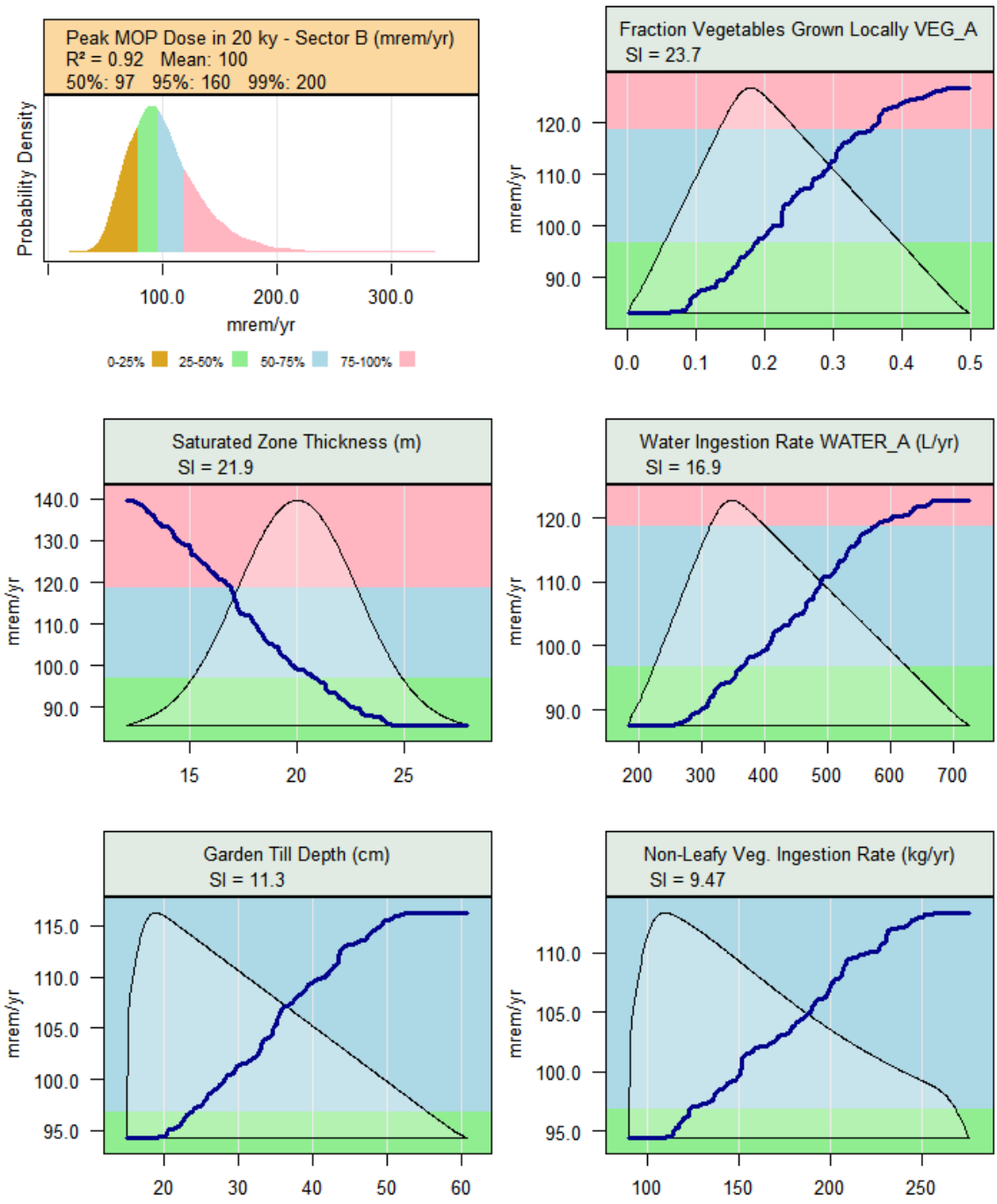

The five most significant sensitive parameters for determining the 10,000-year peak MOP dose for Alternative Sensitivity Case K in Sector G (Figure 2.3-24) are exactly the same as for all sectors (Figure 2.3-20). They reveal Sector G as the one setting the peak dose, consistent with the time histories seen in Figure 2.3-2.

Figure 2.3-24: Probability Density and Partial Dependence of Peak MOP Dose, Sector G within 10,000 Years – Alternative Sensitivity Case K

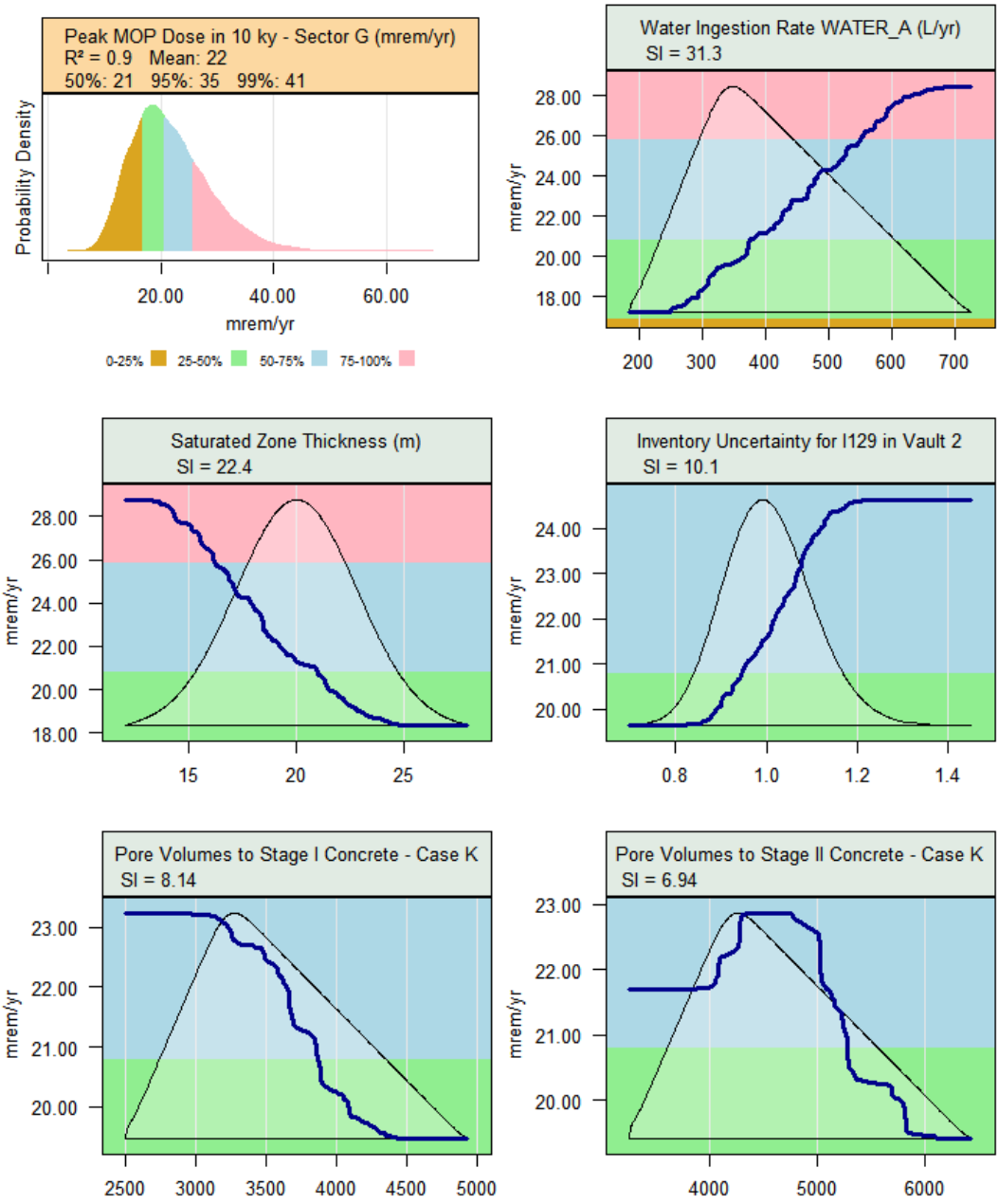

Note: "Pore Volumes to Stage I Concrete" is the number of pore volumes required for concrete to transition from reducing Region II to oxidized Region II. "Pore Volumes to Stage II Concrete" is the number of pore volumes required for concrete to transition from oxidized Region II to oxidized Region III.

Similarly, the sensitive parameters for determining the 20,000-year peak MOP dose for Alternative Sensitivity Case K in Sector G (Figure 2.3-25) are the same as for any sector (Figure 2.3-21). Again, this is to be expected given the ranking of sectors seen in Figure 2.3-2.

Figure 2.3-25: Probability Density and Partial Dependence of Peak MOP Dose, Sector G within 20,000 Years – Alternative Sensitivity Case K

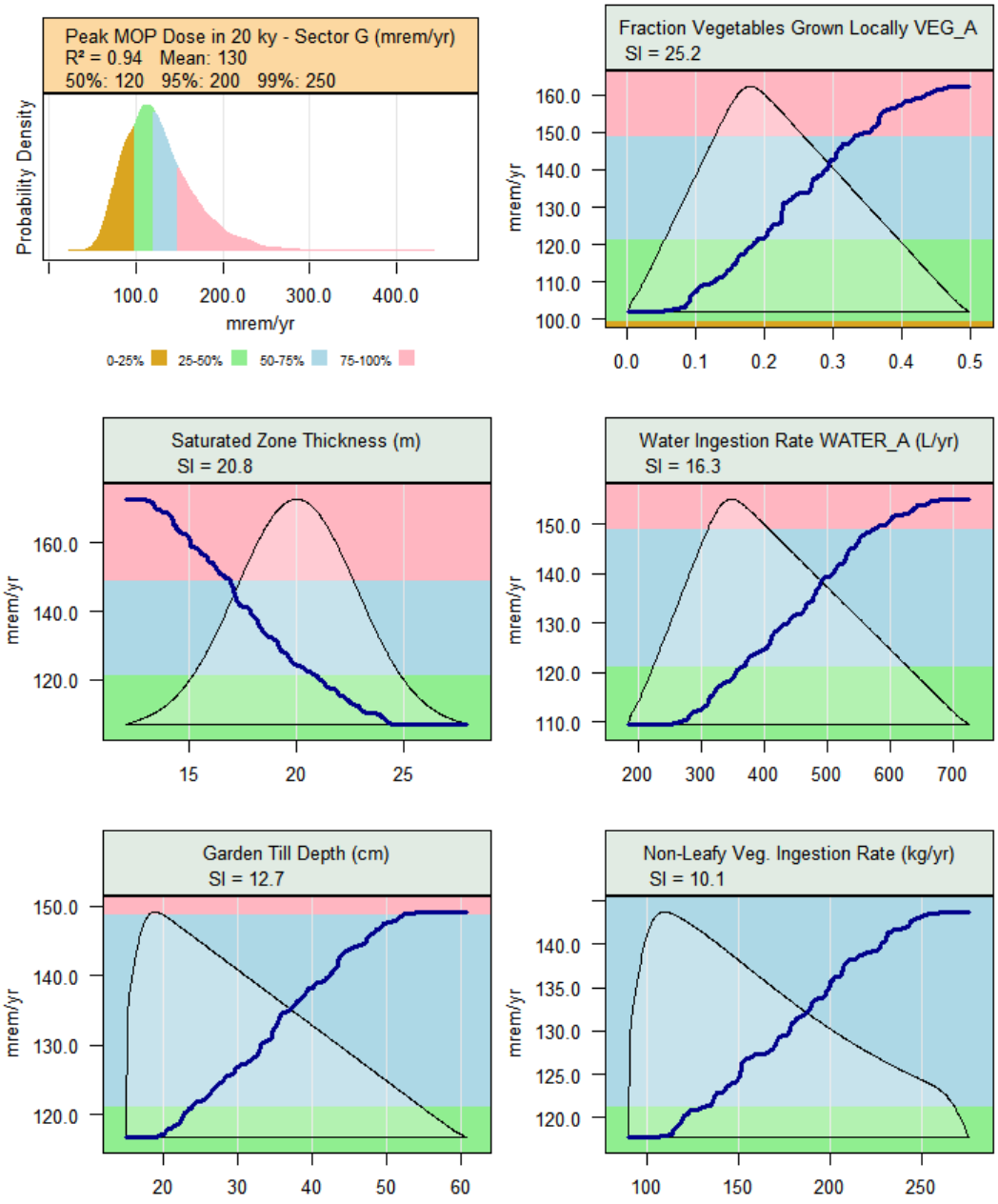

Figure 2.3-26 shows that the most sensitive parameters for Alternative Sensitivity Case K 20,000-year peak concentration of Tc-99 in Sector B are the saturated zone thickness and the uncertainty parameter for the inventory of Tc-99 in the FDCs.

Figure 2.3-26: Probability Density and Partial Dependence of Peak Concentration of Tc-99, Sector B within 20,000 Years – Alternative Sensitivity Case K

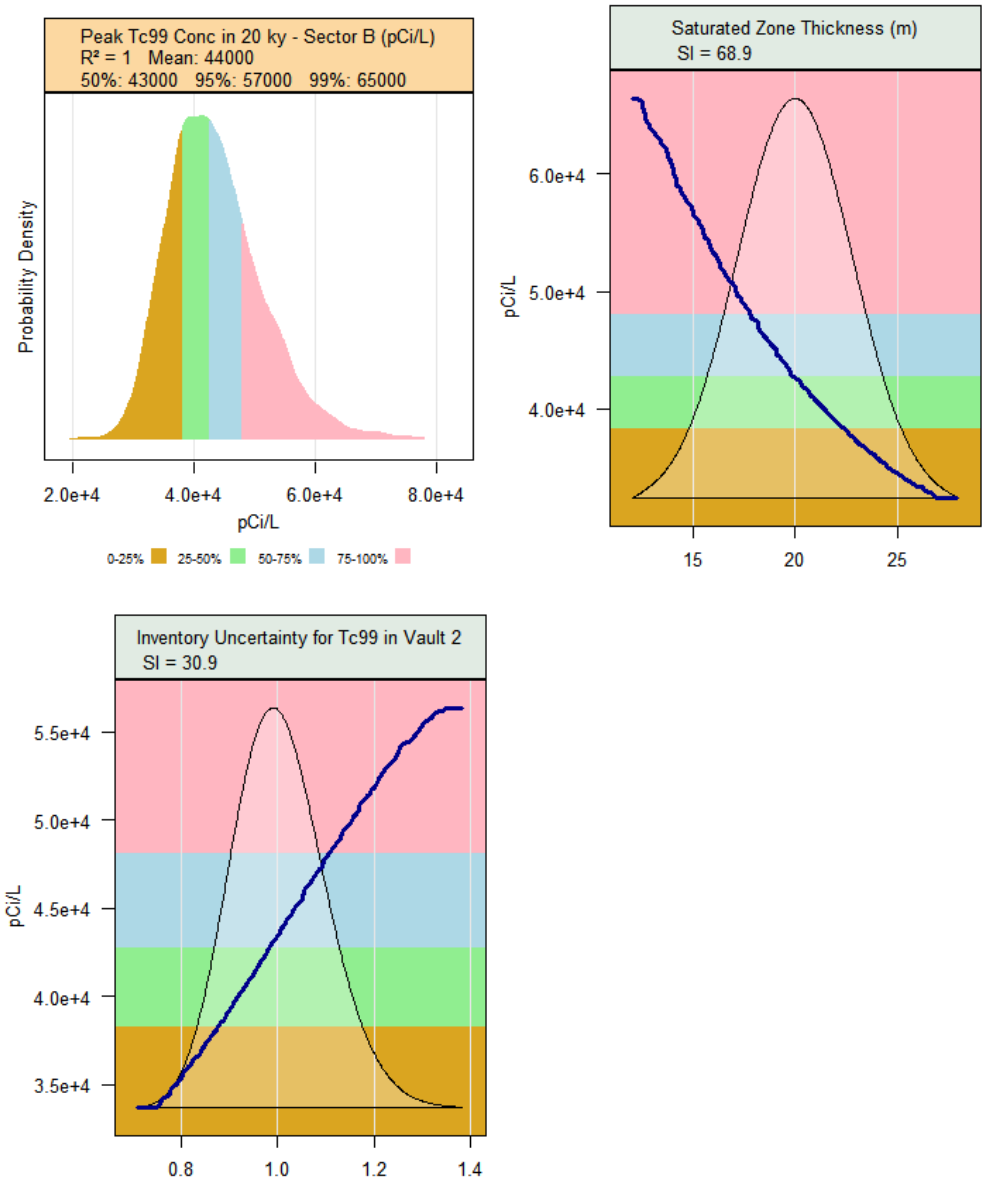

In Figure 2.3-27, the most sensitive parameters for the Alternative Sensitivity Case K 20,000-year peak concentration of Tc-99 in Sector G are the same as those in Sector B (Figure 2.3-26).

Figure 2.3-27: Probability Density and Partial Dependence of Peak Concentration of Tc-99, Sector G within 20,000 Years – Alternative Sensitivity Case K

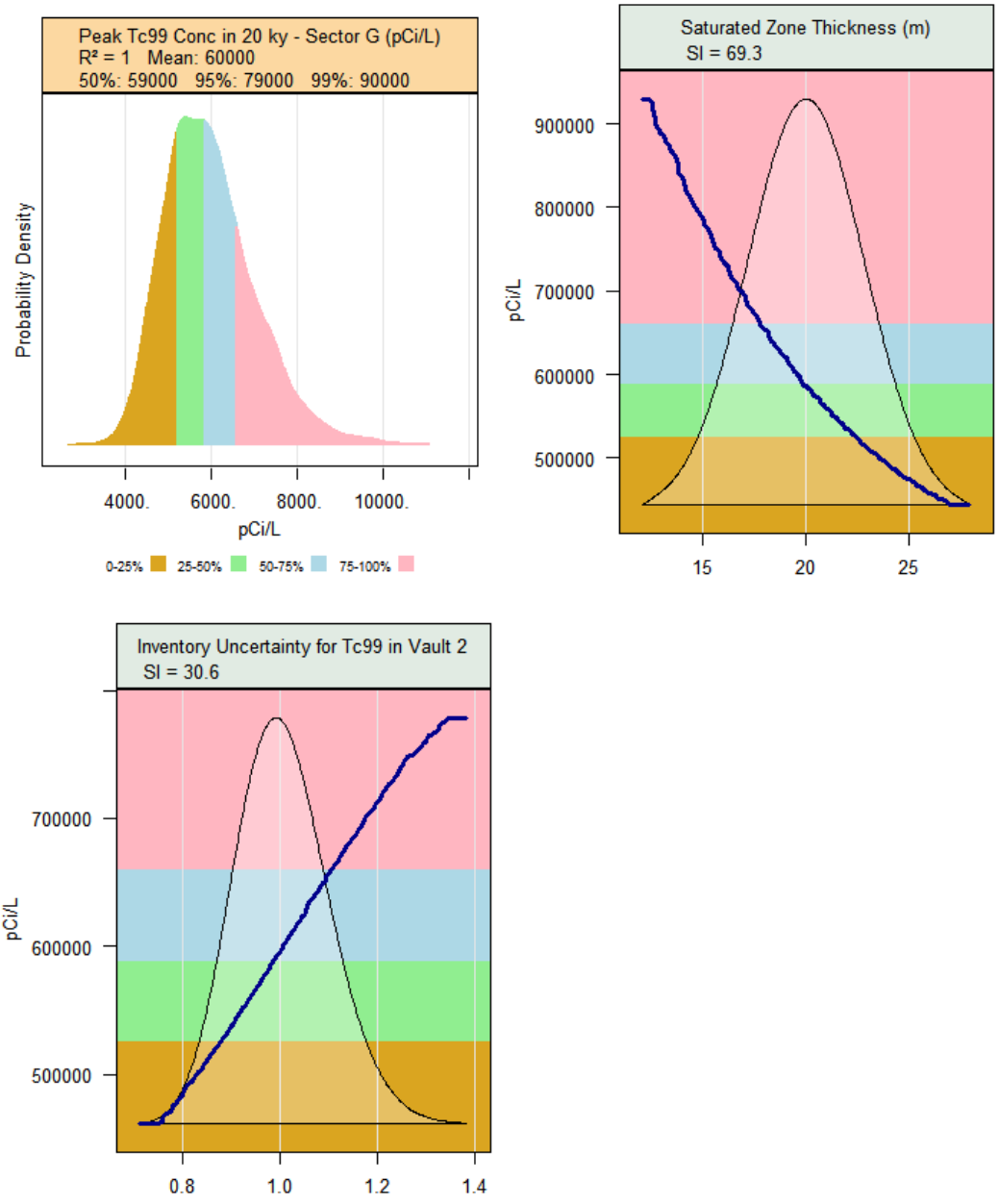

Figure 2.3-28 indicates that the most sensitive parameter for the Alternative Sensitivity Case K 20,000-year peak concentration of I-129 in Sector B is the saturated zone thickness. This is followed by the waste inventory, uncertainty parameter for I-129 in the FDCs, and the required pore volumes for concrete to transition from reducing Region II to oxidizing Region II and from oxidizing Region II to oxidizing Region III.

Figure 2.3-28: Probability Density and Partial Dependence of Peak Concentration of I-129, Sector B within 20,000 Years – Alternative Sensitivity Case K

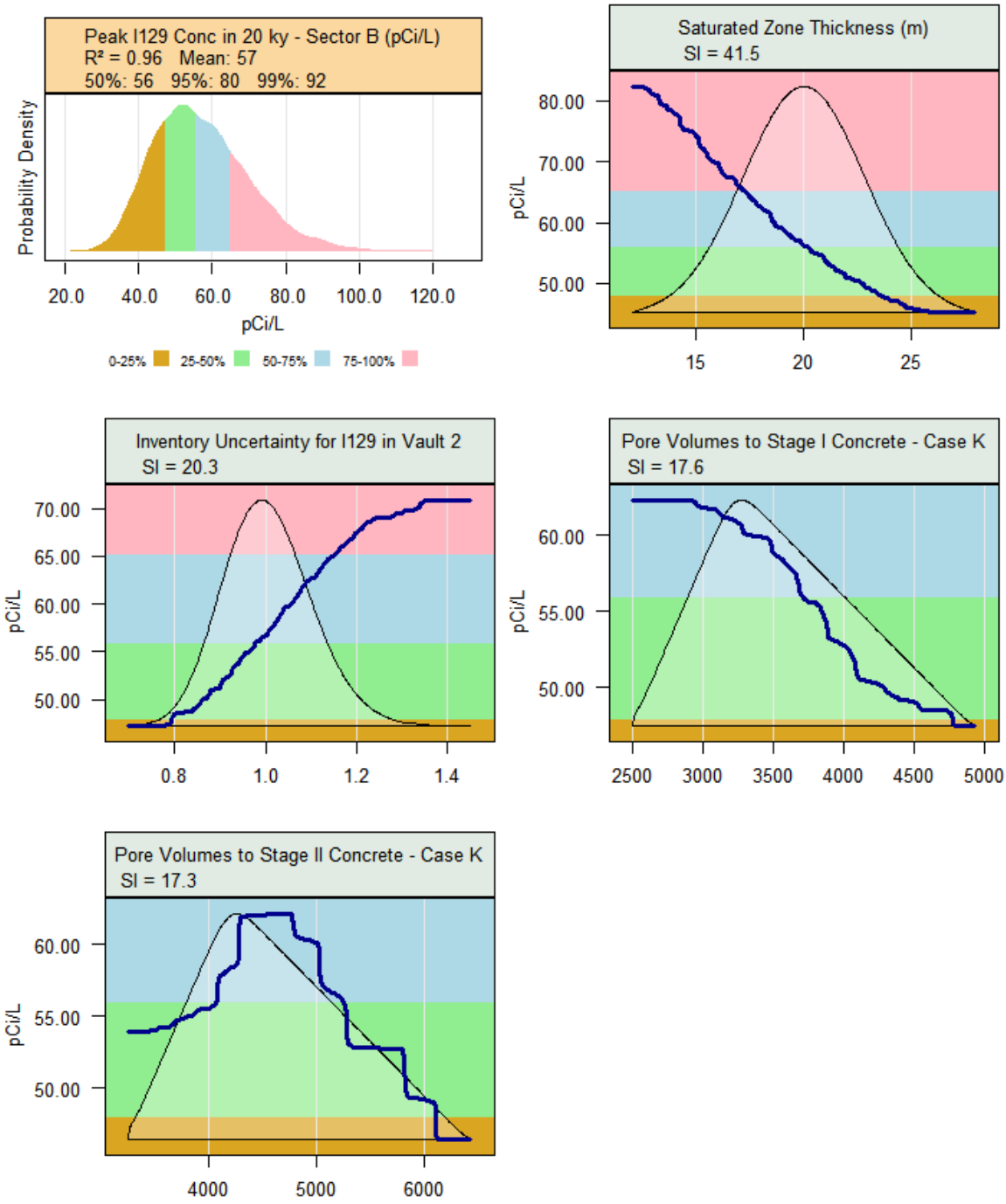

Note: "Pore Volumes to Stage I Concrete" is the number of pore volumes required for concrete to transition from reducing Region II to oxidized Region II. "Pore Volumes to Stage II Concrete" is the number of pore volumes required for concrete to transition from oxidized Region II to oxidized Region III.

Figure 2.3-29 shows that essentially identical influences to those in Sector B (Figure 2.3-28) are found for the Alternative Sensitivity Case K 20,000-year peak concentration of I-129 in Sector G (Figure 2.3-29).

Figure 2.3-29: Probability Density and Partial Dependence of Peak Concentration of I-129, Sector G within 20,000 Years – Alternative Sensitivity Case K

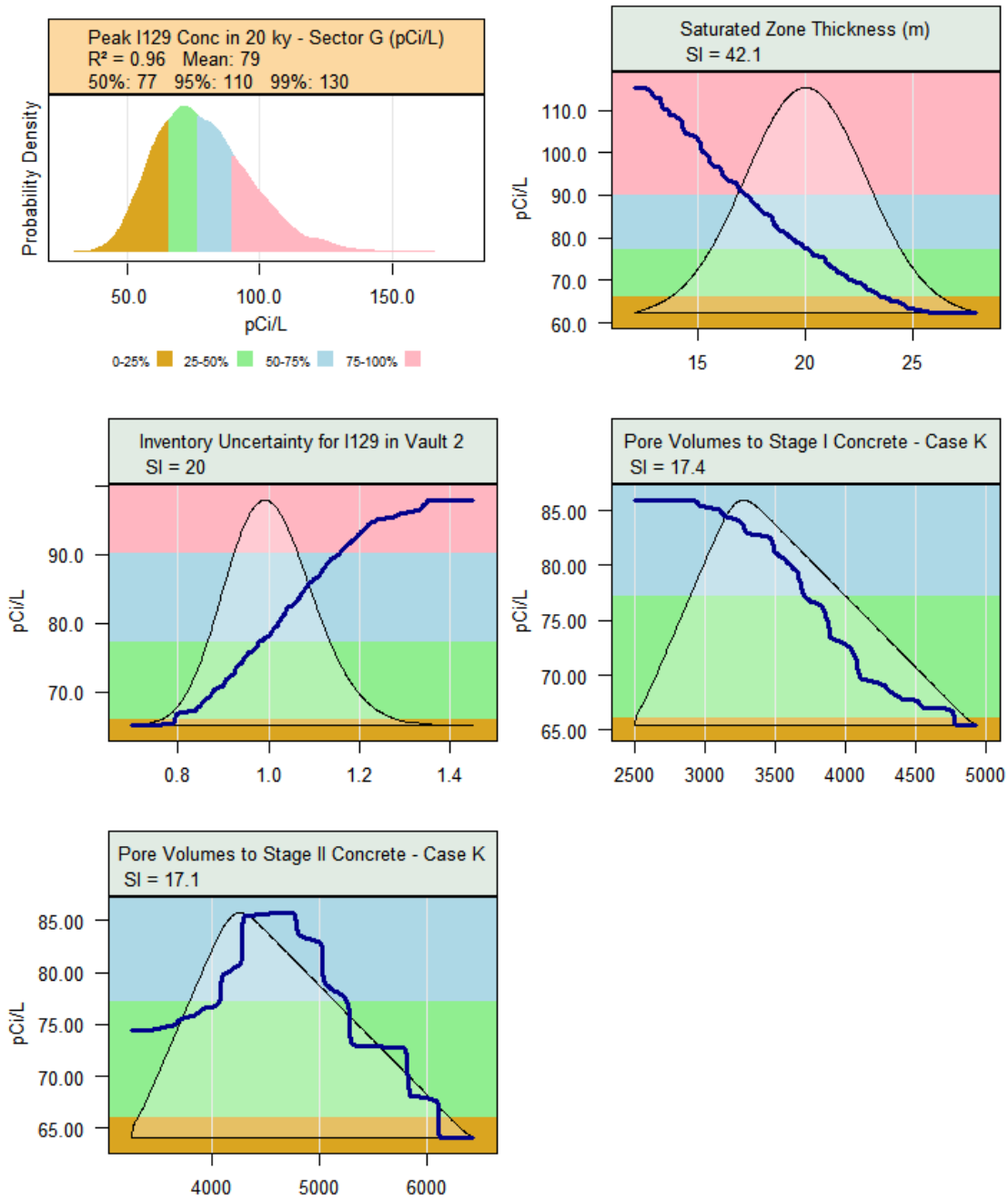

Note: "Pore Volumes to Stage I Concrete" is the number of pore volumes required for concrete to transition from reducing Region II to oxidized Region II. "Pore Volumes to Stage II Concrete" is the number of pore volumes required for concrete to transition from oxidized Region II to oxidized Region III.

For Ra-226, the most sensitive parameter for the Alternative Sensitivity Case K 20,000-year peak concentration of Ra-226 in Sector B is the K_d for radium in sandy soils (Figure 2.3-30), explaining over 80 % of the variation. This is followed by the saturated zone thickness, though it is not nearly as significant.

Figure 2.3-30: Probability Density and Partial Dependence of Peak Concentration of Ra-226, Sector B within 20,000 Years – Alternative Sensitivity Case K

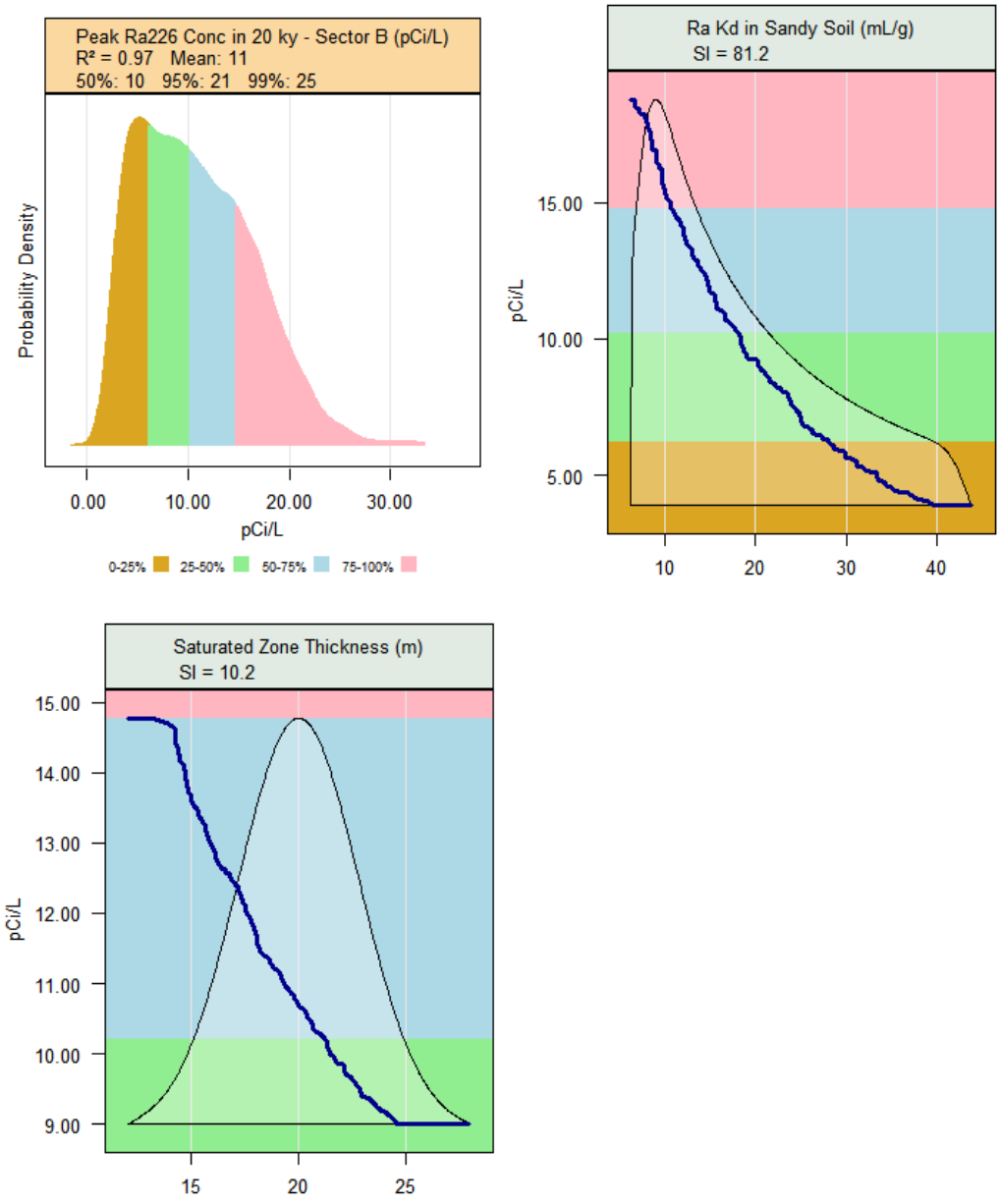

Essentially identical influences to those in Sector B (Figure 2.3-30) are found for the Alternative Sensitivity Case K 20,000-year peak concentration of Ra-226 in Sector G (Figure 2.3-31).

Figure 2.3-31: Probability Density and Partial Dependence of Peak Concentration of Ra-226, Sector G within 20,000 Years – Alternative Sensitivity Case K

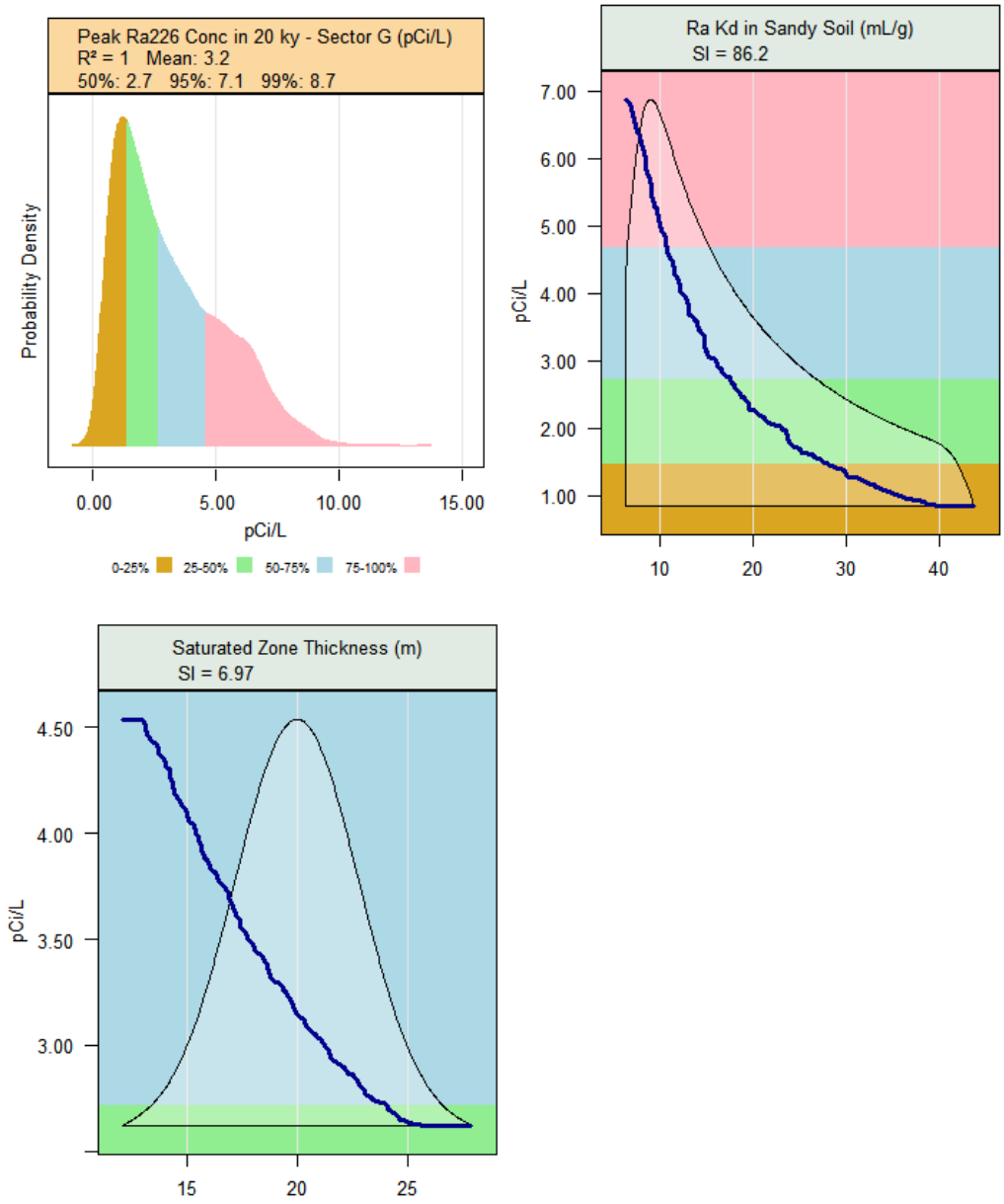

Figure 2.3-32 shows the 20,000-year peak Cs-135 concentration along the streamline is driven by the saturated zone thickness, the cesium K_d in reducing Region II saltstone and reducing Region II floor concrete, and the inventory uncertainty parameter for Cs-135 in Vault 4.

Figure 2.3-32: Probability Density and Partial Dependence of Peak Concentration of Cs-135 Streamline within 20,000 Years – Alternative Sensitivity Case K

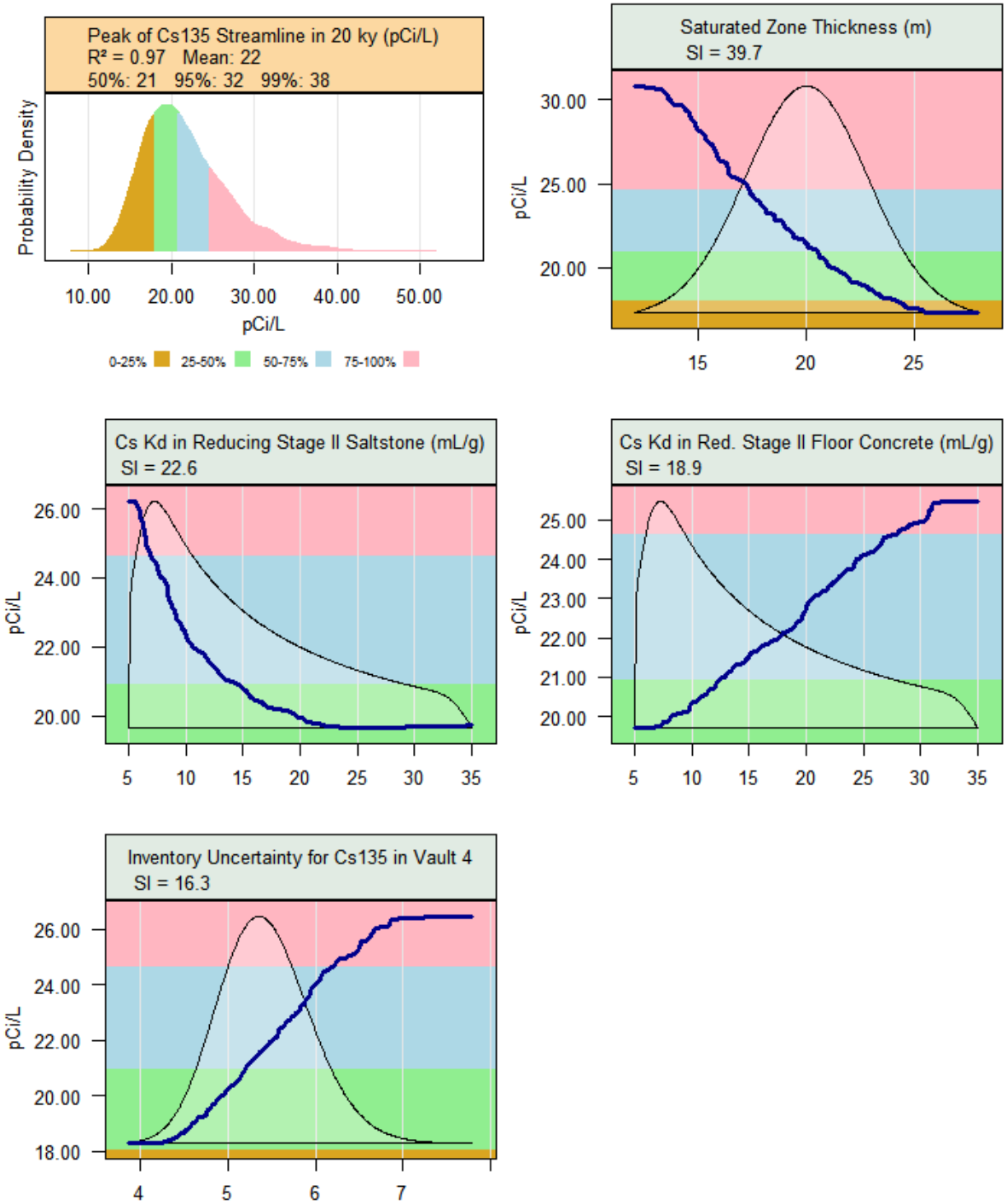

Note: "Cs Kd in Reducing Stage II Saltstone" is the K_d value for cesium in reducing Region II concrete and "Cs Kd in Red. Stage II Floor Concrete" is the K_d value for cesium in reducing Region II floor concrete.

2.3.2.6 Summary of the SDF Probabilistic Model SA

The previous section presented results of the SA for GoldSim v3.001, for configuration SDF PA Case A, and Alternative Sensitivity Case K. Tables 2.3-3 and 2.3-4 summarize the parameters found to be most significant for each endpoint.

Comparison to PA Section 5.6.5.6 and the SDF PA Case A results:

- The thickness of the saturated zone is a significant parameter in both analyses.
- Vegetable production yield or local fraction of vegetables consumed is a significant parameter in the analyses for MOP maximum dose at any sector or at Sector B, for either the 10,000-year or 20,000-year time period.
- Fish ingestion is a significant parameter to the maximum dose to the MOP at Sector J within 10,000 years for both analyses, and within 20,000 years for the SDF PA Case A analysis.
- The significance of the K_d value for iodine that appears in the SDF PA Section 5.6.5.6 analysis, for various endpoints of the maximum dose to the MOP, does not appear in the SDF PA Case A analysis because of model refinements in GoldSim v3.001. The model refinements associated with the reduction in the relative sensitivity of the MOP maximum dose calculations to the K_d for iodine include the increase of the saturated thickness and changes in the saturated zone Darcy velocities. The saturated thickness was increased from 12 to 20 meters in order to reflect more accurately the mixing depth in the PORFLOW simulations. In addition, the saturated zone Darcy velocities were updated to reflect disposal cell specific values derived using a PORFLOW based particle-tracking analysis (see Appendix A in SRR-CWDA-2011-00178).

Comparison to the SDF PA Case A and the Alternative Sensitivity Case K results:

- An expected common thread between the two analyses is the significance of the thickness of the saturated zone.
- Because of changes to inventory and K_d values made in Alternative Sensitivity Case K, Ra-226 is not a significant contributor to dose and thus parameters associated with radium are not significant to endpoints associated with the maximum dose to the MOP for Alternative Sensitivity Case K.
- The significant contributor to the MOP dose within 10,000 years for Alternative Sensitivity Case K is I-129 as indicated by the significance shown for the I-129 inventory uncertainty, and pore volumes necessary for concrete transitions.

- Because of model refinements made in Alternative Sensitivity Case K to implement the Tc-99 release "shrinking core" model, the sensitive parameters for the Tc-99 concentration do not include the SDF PA Case A sensitive parameters of technetium K_d value in reducing moderate age concrete and pore volumes necessary for concrete transitions.
- Because of the aggressive degradation rate of cementitious materials in Alternative Sensitivity Case K, much greater flow occurs throughout the closure system than what occurs in SDF PA Case A; therefore, for Alternative Sensitivity Case K the sensitive parameters for the concentration of I-129 include the pore volumes necessary for concrete transitions.

2.3.2.7 Conclusions

The UA/SA conducted using GoldSim v3.001 provided expected results for SDF PA Case A and Alternative Sensitivity Case K, and is representative of the SDF conceptual model.

3.0 REFERENCES

ISSN 0885-6125 Vol. 24 No. 2, (Copyright), Breiman, L., *Bagging Predictors*, University of California, Berkeley, November 21, 1995.

ISSN 0885-6125 Vol. 40 No. 2, (Copyright), Dietterich, T.G., *An Experimental Comparison of Three Methods for Constructing Ensembles of Decision Trees*, Oregon State University, Corvallis, OR, January 1, 2000.

ML083190829 (Copyright), *Description of Methodology for Biosphere Dose Model BDOSE,* U.S. Nuclear Regulatory Commission, Washington DC, November 30, 2008.

ML100820097, *Request for Additional Information on the 2009 Performance Assessment for the Saltstone Disposal Facility at the Savannah River Site*, U.S. Nuclear Regulatory Commission, Washington DC, March 2010.

ML103400571, *Second Request for Additional Information on the 2009 Performance Assessment for the Saltstone Disposal Facility at the Savannah River Site, Docket Number PROJ0734,* (Enclosure RAI-2009-01 included), U.S. Nuclear Regulatory Commission, Washington DC, December 13, 2010.

RAI-2009-02, *Second Request for Additional Information for the 2009 Performance Assessment for the Saltstone Disposal Facility at the Savannah River Site (ML103400571 Enclosure)*, U.S. Nuclear Regulatory Commission, Washington DC, March 2010.

SRNL-STI-2010-00447, Jannik, G.T., et al., *Land and Water Use Characteristics and Human Health Input Parameters for Use in Environmental Dosimetry and Risk Assessments at the Savannah River Site*, Savannah River Site, Aiken, SC, Rev. 0, August 6, 2010.

SRR-CWDA-2009-00017, *Performance Assessment for the Saltstone Disposal Facility at the Savannah River Site*, Savannah River Site, Aiken, SC, Rev. 0, October 2009.

SRR-CWDA-2010-00033, *Comment Response Matrix for Nuclear Regulatory Commission (NRC) Requests for Additional Information (RAIs) on the Saltstone Disposal Facility Performance Assessment (SRR-CWDA-2009-00017, Revision 0, dated October 29, 2009),* Savannah River Site, Aiken, SC, Rev. 1, July 23, 2010.

SRR-CWDA-2011-00044, *Comment Response Matrix for Nuclear Regulatory Commission RAI-2009-02 Second Request for Additional Information (RAI) on the Saltstone Disposal Facility Performance Assessment (SRR-CWDA-2009-00017, Revision 0, dated October 29, 2009)*, Savannah River Site, Aiken, SC, Rev. 0, April 2011.

SRR-CWDA-2011-00044, *Comment Response Matrix for Nuclear Regulatory Commission RAI-2009-02 Second Request for Additional Information (RAI) on the Saltstone Disposal Facility Performance Assessment (SRR-CWDA-2009-00017, Revision 0, dated October 29, 2009)*, Savannah River Site, Aiken, SC, Rev. 1, August 2011.

SRR-CWDA-2011-00178, *Saltstone Disposal Facility Stochastic Fate and Transport Model*, Savannah River Site, Aiken, SC, January 2012.

SRR-CWDA-2011-00189, *SRS Saltstone v3.002.gsm*, Savannah River Site, Aiken, SC, November 2011.